ROBUST FEDERATED LEARNING WITH MAJORITY ADVERSARIES VIA PROJECTION-BASED RE-WEIGHTING

Anonymous authors
Paper under double-blind review

ABSTRACT

Most robust aggregators for distributed or federated learning assume that adversarial clients are the minority in the system. In contrast, this paper considers the majority adversary setting. We first show that a filtering method using a few trusted clients can defend against many standard attacks. However, a new attack called Mimic-Shift can circumvent simple filtering. To this end, we develop a re-weighting strategy that identifies and down-weights the potential adversaries under the majority adversary regime. We show that our aggregator converges to a neighborhood around the optimum under the Mimic-Shift attack. Empirical results further show that our aggregator achieves negligible accuracy loss with a majority of adversarial clients, outperforming strong baselines.

1 INTRODUCTION

Federated learning (FL) is a leading framework for collaboratively training a machine learning (ML) model over local datasets. The decentralized nature of FL systems has raised concerns about vulnerability – as adversaries can connect to an FL system like other benign users and corrupt the ML model while evading detection by standard means (Kairouz et al., 2021). To this end, there is growing literature on the adversarial robustness of FL (Blanchard et al., 2017; Chen et al., 2018; Xie et al., 2019b; Rajput et al., 2019b; Xie et al., 2020; Karimireddy et al., 2021a; 2022; He et al., 2022b), particularly where adversaries can upload malicious updates. Most existing defenses assume that the adversarial clients are the minority in the system (Blanchard et al., 2017; Chen et al., 2018; Rajput et al., 2019b; Karimireddy et al., 2021a; He et al., 2022b). However, in a federated scenario, the decentralized nature means that it is relatively straightforward for the adversary to be the majority and thus break existing defenses. We call such an adversary the "majority adversary".

Our work joins a growing literature on robustness with majority adversaries, e.g., Xie et al. (2019b; 2020), motivated by noted practical vulnerabilities. Although Shejwalkar et al. (2021) argue that the number of registered clients in a production system (e.g., GBoard) may be too large for the adversary to compromise a majority of them, they neglect the client availability issue in FL. In particular, Kairouz et al. (2021) suggests that, at any given time, only a subset ($< 1\%$) of clients are available for the server. Such a low client availability allows the adversary to become the majority and overwhelm the server utilizing compromised networked devices (e.g., IoT devices) in a similar way as the common distributed denial-of-service (DDoS) attack (Specht & Lee, 2003; Bonguet & Bellaïche, 2017). Some other settings such as crowd-sourced training (Ryabinin & Gusev, 2020) (a.k.a. volunteer computing) are perhaps even more vulnerable to majority adversaries because the crowd-sourcing systems do not implement access control – allowing the adversary to connect an arbitrary number of clients as volunteers.

We consider the adversarial robustness of federated learning against a class of attacks where an adversary aims to decrease the accuracy of the trained ML model by uploading malicious updates. In particular, we are interested in Mimic-type attacks (Karimireddy et al., 2022), as is discussed later in this section. A key assumption in our setup is the existence of a few trusted clients, e.g., with secure hardware support. We call these trusted clients "reference clients". In practice, the number of reference clients could be as small as two in each round. Similar approaches have been considered in existing works (Xie et al., 2019b; 2020). One option for secure hardware is the trusted execution environment (TEE) (Pinto & Santos, 2019), which guarantees that the program is not Byzantine. TEE is so far commercialized (e.g., on Google Pixel (GoogleBlog), Apple iPhone (AppleSupport), Sam-

sung phones (SamsungDeveloper)). Recent works (Mo et al., 2021) bring TEE support to federated learning systems.

We propose a combination of defenses – filtering and projection-based re-weighting. Our first defense is a filtering method that constructs a spherical accept region and excludes the updates outside it. The center of the accept region is an average update from a few trusted clients with secure hardware support. The radius of the accept region is the sample variance of reference updates times a scaling factor. Although the filtering method is effective against several standard attacks (e.g., sign flipping attack, Gaussian attack), this filtering is easy to circumvent.

Building on the recently proposed Mimic attack (Karimireddy et al., 2022), shown to break many existing defenses, we develop an improved attack method called Mimic-Shift. Mimic-Shift clients send malicious updates which slightly shift away from benign updates and mislead the aggregated updates away from the expected update. The slight shift makes Mimic-Shift hard to detect, and the calibrated shifting direction can corrupt the aggregated model. To perform the Mimic-Shift attack, we consider a man-in-the-middle (MITM) adversary capable of intercepting the message between the clients and the server. Computer security researchers have extensively studied the MITM adversary, but existing encryption solutions can be too expensive for resource-constrained client devices. For example, the AES (advanced encryption standard) encryption only has a throughput of around 50 MB/s even with a powerful desktop CPU (Gleeson et al., 2014). With a 1 GB moderate size neural network, the encryption takes more than 20 seconds on the client-side, draining the computational resources and increasing the client dropout rate.

Our second defense is a projection-based re-weighting method to deal with the Mimic-Shift attack under a majority adversary regime. The main idea is to measure the influence of each update on the aggregated update, then down-weight the updates with high influence. Specifically, we compute the scalar projection of the aggregated update on each client's update. The intuition is that the majority adversarial clients can significantly mislead the aggregated update, resulting in a large scalar projection. Note that the filtering and re-weighting methods complement each other because the re-weighting defense does not deal with the aforementioned standard attacks, as is discussed in Section 4.

We further provide some theoretical analysis of our methods under the Mimic-Shift attack. First, false-positives in filtering can eliminate a benign update and perturb the aggregated update. Regarding this concern, we show that the false positive rate decreases quickly w.r.t. the number of reference clients and the scaling factor of the accept radius, suggesting that our filtering method can work with a few reference clients and a conservative scaling factor. For the re-weighting phase, the probability of malicious updates having larger scalar projections than benign updates increases as the adversary takes more shares in a system, complementing existing results (He et al., 2022b) that guarantee more robustness as the share of the adversary decreases. Additionally, we discuss the performance of our method under a conventional minority adversary setting. Finally, we show that, in a convex setting, our method converges with a rate of $\mathcal{O}(\frac{1}{\sqrt{T}})$ to a neighborhood of the optimum. Our contributions are summarized as follows:

- We develop the Mimic-Shift attack and show that Mimic-Shift circumvents many defense methods in federated learning.
- We develop a two-stage defense using filtering and re-weighting to defend against a broad class of attacks.
- We theoretically analyze our strategy and outline conditions under which it helps.

Empirical results on FEMNIST (Caldas et al., 2018), CelebA (Liu et al., 2015) and Shakespeare (McMahan et al., 2017) datasets show that our aggregator recovers a near-optimal model under a majority adversary setting with Mimic-Shift attack, outperforming existing methods by a large margin. Also, our method only loses up to 2.4% accuracy under conventional minority adversary settings. Additional empirical results demonstrate that our method is robust to a broad class of attacks, including standard Gaussian and sign-flipping attacks as well as an improved Mimic-Shift-Var attack.

2 RELATED WORK

Many existing works on Byzantine robust machine learning assume the adversary is the minority in the system, based on clustering (Blanchard et al., 2017), median (Yin et al., 2018), voting (Bernstein et al., 2019), bucketing (Karimireddy et al., 2022), and robust estimation (Data & Diggavi, 2021). However, these methods can fail once the adversary becomes the majority. A few papers (Xie et al., 2019b; 2020) leverage a validation dataset to improve Byzantine tolerance to arbitrary numbers of adversarial clients but constructing a global validation dataset in a federated scenario with local private datasets is infeasible. Other redundancy-based methods with more robustness guarantees do not apply to federated learning because they assume a centralized setting with control over the data allocation on each node (Chen et al., 2018; Rajput et al., 2019a). Recently, a clipping-based method (Karimireddy et al., 2021b; He et al., 2022b) showed success against minority adversary in a federated learning setting. Although it is relatively straightforward to combine the clipping with our reference clients, we find that the training is unstable, as is discussed in Section 6.

Our paper focuses on model poisoning attacks, which aim to decrease the accuracy of the trained ML model by uploading malicious updates (He et al., 2022b). Other attacks, including data poisoning (Steinhardt et al., 2017; Wang et al., 2021) and backdoor (Wang et al., 2020; Xie et al., 2021), are beyond the scope of this work. We focus only on training the centralized model. Additional considerations such as personalization are known to be handled effectively using robust centralized training, followed by local fine-tuning Li et al. (2021), thus are beyond the scope of this paper.

3 PROBLEM SETUP

We assume a federated learning system where N benign clients collaboratively train a ML model $f : \mathcal{X} \to \mathcal{Y}$ with d-dimensional parameter ζ coordinated by a server. The N benign clients include N_R reference (trusted) clients. There are N' adversarial clients who aim to corrupt the ML model during training. The i^{th}, $i \in [1, ..., N + N']$, client has n_i data samples, being benign for $i \in [1, ..., N]$ or being adversarial for $i \in [N + 1, ..., N + N']$. The federated learning is conducted in T rounds. In round $t \in [1, ..., T]$, the server broadcasts a model parameterized by ζ_{t-1} to each client. We omit the subscript t while focusing on one round. Then, the i^{th} client optimizes ζ_{t-1} with their local data samples and report $\zeta_{t,i}$ to the server. We define pseudo-gradient $g_{t,i} = \zeta_{t-1} - \zeta_{t,i}$ being the difference between the locally optimized model and the broadcasted model from the previous round. Note, for simplicity, that we will often use the term "gradient" to refer to the updates. Once all the gradients are reported in, the server aggregates the gradients and produce a new model with parameters ζ_t using the following rule: $\zeta_t = \zeta_{t-1} - \sum_{i=1}^{N+N'} \frac{n_i}{\sum_{i=1}^{N+N'} n_i} g_{t,i}$. Our goal is to minimize a risk function over the benign clients: $F(\zeta) = \sum_{i=1}^{N} \frac{n_i}{\sum_{i=1}^{N} n_i} F_i(\zeta) = \sum_{i=1}^{N} \frac{n_i}{\sum_{i=1}^{N} n_i} \mathbb{E}_{\mathcal{D}_i}[\ell(f(x; \zeta), y)]$, where $\ell : \mathbb{R} \times \mathcal{Y} \to \mathbb{R}$ is a loss function.

3.1 THREAT MODEL

Following the standard practice (Blanchard et al., 2017), we consider an omniscient man-in-the-middle (MITM) adversary that knows $g_i, \forall i \in \{1, ..., N\}$ and can tell which clients are reference users, e.g., by observing the device identifier in the message. An omniscient adversary helps explore the limits of the defense. However, an omniscient adversary is not mandatory for our Mimic-Shift attack, which can work with partial information as Section 6 will show. The MITM adversary also owns a majority of clients in a system and adopts an attack from the Mimic family (Karimireddy et al., 2022). Specifically, we assume the following Mimic-Shift attack.

Mimic-Shift At each round, the MITM adversary first intercepts the gradients from benign clients. Then the adversary computes the average reference gradient $\bar{g}_R = \sum_{i=1}^{N_R} \frac{n_{R_i}}{\sum_{i=1}^{N_R} n_{R_i}} \cdot g_{R_i}$ from the reference users indexed by R_i and the average benign gradient $\bar{g} = \sum_{i=1}^{N} \frac{n_i}{\sum_{i=1}^{N} n_i} \cdot g_i$ from all benign users, including the reference users. Then, all the adversarial clients report $g' = \bar{g}_R + (\bar{g}_R - \bar{g})$ to the server.

The Mimic-Shift attack is effective because it tries to push the aggregated gradient away from the expected gradient. The reason is that $\bar{g}$ is estimated with more clients and data samples. A simple concentration argument suffices to show that $\bar{g}$ will be closer to $\mathbb{E}[\bar{g}]$ than $\bar{g}_R$ with high probability,

resulting in a $\bar{g}_R - \bar{g}$ pointing away from $\mathbb{E}[\bar{g}]$. Empirical results in Section 6 show that Mimic-Shift decreases the accuracy twice as much as Mimic (Karimireddy et al., 2022), which sets $g' = g_i$ for an $i \in \{1, ..., N\}$.

The Mimic-Shift attack is also difficult to detect because the malicious g' has the same distance to the reference $\bar{g}_R$ as the benign $\bar{g}$. We will see how this property lets Mimic-Shift bypass distance-based defenses in Section 6.

4 METHOD

Our robust aggregator has two phases, filtering and re-weighting. The filtering phase, applied first, excludes the gradients outside the accept region defined by the reference gradients, defending against standard attacks. Then, the re-weighting phase further down-weights the potential malicious gradients within the accepting region of the filtering phase, targeting the Mimic-Shift attack.

4.1 PHASE 1: FILTERING

In the filtering phase (Algorithm 1), we first compute the sample mean of reference gradient $m_R = \sum_{i=1}^{N_R} \frac{1}{N_R} \cdot g_{R_i}$, making a guess of where the good gradients might be. Next, we set m_R as the center of a spherical accept region. Then, we compute the sample variance of the reference gradients, $s_R = \frac{\sum_{i=1}^{N_R} \|g_{R_i} - m_R\|}{N_R - 1}$. The sample variance s_R is further scaled up by a tunable hyper-parameter c. The product $c \cdot s_R$ is the radius of the spherical accept region. Finally, we remove all the updates outside the spherical accept region. This filtering is effective against attacks that do not know where the expected gradient is (e.g., Gaussian attack) or do not carefully calibrate the adversarial gradient (e.g., sign flipping attack), as is shown in Section 6.

Algorithm 1 Filtering.

Input:
A set of reference gradients, $\{g_{R_i} \mid i \in \{1, ..., N_R\}\}$;
A set of reported gradients, $\{g_i \mid i \in \{1, ..., N + N'\}\}$;
A hyper-parameter c;

Aggregator:
1: Compute the sample mean of reference gradients, $m_R := \sum_{i=1}^{N_R} \frac{1}{N_R} \cdot g_{R_i}$;
2: Compute the sample variance of reference gradients, $s_R := \frac{\sum_{i=1}^{N_R} \|g_{R_i} - m_R\|}{N_R - 1}$;
3: **return** $\{g_i \mid i \in \{1, ..., N + N'\} \wedge \|g_i - m_R\| \leq c \cdot s_R\}$;

4.2 PHASE 2: RE-WEIGHTING

Suppose a majority adversary misleads the aggregated gradient. In that case, the malicious gradients likely have a stronger influence on the aggregated gradient compared to benign gradients. Here, we measure the influence via scalar projections.

The re-weighting defense is outlined in Algorithm 2. The scaling weights are designed to augment benign gradients and down-weight adversarial updates. This is implemented using a monotonic re-scaling [1] of the scalar projection between the aggregate and the gradients (step 4). The monotonic re-scaling amplifies the difference between the scalar projections, making large projections larger. Therefore, the potential malicious gradients would be down-weighted more. However, the monotonic re-scaling may also lead to an over-up-weighting on certain benign gradients, which are far from $\bar{g}^*$. such up-weighting leads to instability in the training process. Thus, we also include a clipping operator (step 6). The clipping addresses the over-up-weighting issue by specifying a bound.

An additional benefit of using the power function and clipping is that they prompt a set of uniform weights on benign gradients, stabilizing the training. If we set k to be sufficiently large such that the maximum s_i is greater than $N_F \cdot (\sum_{i=1}^{N_F} s_i - \max_{i \in \{1,...,N_F\}} s_i)$, we have $s_i = \tau, \forall i \neq$

[1] In the description and experiments, we use a power function. Optimizing the choice of monotonic re-scaling is left for future work.

$\arg\max_{i \in \{1,...,N_F\}} s_i$. In practice, we set k to 10 and τ to 0.6. Both hyper-parameters generalize well to the three datasets in our experiments.

Note that the filtering phase complements the re-weighting phase because standard attacks can corrupt the scalar projections via uploading 0 or flipping the sign. For a class of inner product-based attacks (Xie et al., 2019a), an additional clipping operator that prevent the scalar projection s_i from being negative can help.

Algorithm 2 Re-weighting.

Input:
A set of filtered gradients, i.e., the results of Algorithm 1, $\{g_i \mid i \in \{1, ..., N_F\}\}$;
Two hyper-parameters k and τ;
Aggregator:
Compute the aggregated gradients of all users, $\bar{g}^* := \sum_{i=1}^{N_F} \frac{n_i}{\sum_{i=1}^{N_F} n_i} g_i$;
Compute a scalar projection of $\bar{g}^*$ on each g_i, $s_i := \frac{\bar{g}^* \cdot g_i}{\|g_i\|}$;
Normalize the vector $s = [s_1, ..., s_{N_F}]$ such that $\|s\|_1 = N_F$;
Take the k^{th} power of each s_i, $s := [s_1^k, ..., s_{N_F}^k]$;
Normalize the vector $s = [s_1, ..., s_{N_F}]$ such that $\|s\|_1 = N_F$;
Clip the values smaller than τ in s, $s_i := \max(s_i, \tau), \forall i \in \{1, ..., N_F\}$;
Normalize the vector $s = [s_1, ..., s_{N_F}]$ such that $\|s\|_1 = N_F$;
Re-weight each g_i using s_i, $g_i := \frac{g_i}{s_i}, \forall i \in \{1, ..., N_F\}$;
return $\bar{g}j := \sum_{i=1}^{N_F} \frac{n_i}{\sum_{i=1}^{N_F} n_i} g_i$;

5 Theoretical Analysis

We first show that the probability of not filtering out a benign gradient increases at a rate of $\mathcal{O}(1 - \frac{1}{N_R^2})$ w.r.t. the number of reference clients N_R and $\mathcal{O}\big((1 - \frac{1}{c^2})^2\big)$ w.r.t. the scaling factor c in the accept radius. Then, we discuss conditions for the probability of down-weighting the malicious gradients to increase as the adversary owns more clients in the system. Additional discussion considers how our strategy may still help even if the aforementioned conditions do not hold, providing insights to certain of empirical results. Finally, we study the convergence of our method under a convex setting. Before proceeding, we outline some additional assumptions.

To simplify tedious notation, we assume all users have the same number of samples because the difference in sample size can be merged into the difference between gradients.

Assumption 1. *Uniform sample size:*

$$n_i = n_j, \forall i \neq j. \tag{1}$$

Assumption 2. *The gradients follow a hierarchical distribution in all rounds:*

$$\begin{aligned} &\text{Stage 1} : \mu_i \sim P(\mu), \sigma_i \sim P(\sigma), \forall i \in \{1, ..., N\}, \\ &\text{Stage 2} : g_i \sim \mathcal{N}(\mu_i, \sigma_i; \gamma^+), \forall i \in \{1, ..., N\}, \end{aligned} \tag{2}$$

where Stage 1 is a distribution where the random variable μ has finite expected value $\mathbb{E}[\mu]$ and finite non-zero variance $\text{Var}[\mu]$. *Stage 2 is truncated isotropic Gaussian distribution with a truncation threshold γ^+ on the L_2 norm.*

Assumption 3. *The variance of gradients is bounded:*

$$\sigma_i \leq \sigma^+, \forall i \in \{0, 1, ..., N\}. \tag{3}$$

Assumption 4. *The sample variance of reference gradients is greater than 0:*

$$0 < s_R^- \leq s_R. \tag{4}$$

Assumption 5. *The L_2 norm of expected and estimated gradients is bounded:*

$$\begin{aligned} &0 < \gamma^- \leq \|\mu_i\| \leq \gamma^+, \forall i \in \{0, 1, ..., N\}, \\ &0 < \gamma^- \leq \|g_i\| \leq \gamma^+, \forall i \in \{0, 1, ..., N\}. \end{aligned} \tag{5}$$

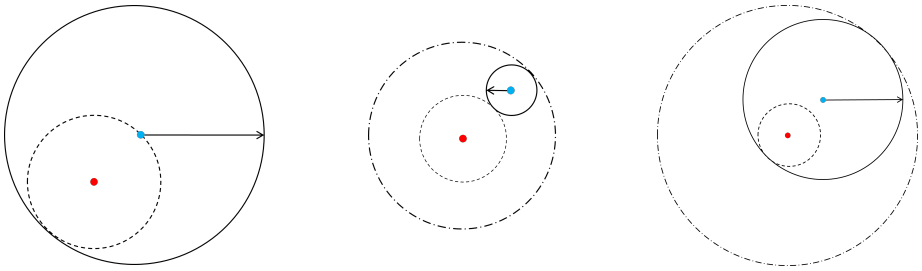

(a) Case 1. (b) Case 2. (c) Case 3.

Figure 1: Three cases with different hyper-parameters c. The red dot is $\mathbb{E}[\mu]$ and the blue dot is $\bar{\mu}_R$. The solid circle represents the accept region with radius $c \cdot s_R$. The dash circle and dash dot circle(s) are two spherical contours around $\mathbb{E}[\mu]$. Condition $c \geq 2 \cdot \frac{\|\mathbb{E}[\mu]-\bar{\mu}\|}{s_R}$ holds in Case 1, where all the points outside the accept region are more than $\frac{c \cdot s_R}{2}$ away from $\mathbb{E}[\mu]$. In Case 2 and Case 3, there are points between the two contours that have the same distance to $\mathbb{E}[\mu]$ but are not always inside accept region.

5.1 Filtering (Stage 1)

The filtering phase removes all the gradients that are more than $c \cdot s_R$ away from the reference m_R in terms of Euclidean distance. However, the data distribution $\mathcal{D}_i$ may vary across clients in a federated learning setting. Such non-i.i.d.ness increases the risk of filtering out a benign gradient. We start our analysis by considering the expected gradients:

Lemma 6. *Suppose there are N_R reference clients among N clients, and the sample variance of gradients is s_R, under Assumption 2, let $c \geq 2 \cdot \frac{\|\mathbb{E}[\mu]-\bar{\mu}\|}{s_R}$. Then, for any $i \in [1, ..., N]$, with probability at most $\frac{4 \cdot \mathrm{Var}[\mu]^2}{c^2 \cdot s_R^2}$, we have $\|\mu_i - \bar{\mu}_R\| \geq c \cdot s_R$, where $\bar{\mu}_R = \sum_{i=1}^{R} \frac{1}{N_R} \cdot \mu_{R_i}$.*

Remark 7. *Condition $c \geq 2 \cdot \frac{\|\mathbb{E}[\mu]-\bar{\mu}\|}{\mathrm{Var}[\mu]}$ guarantees that all μ_is outside the accept region are at least $\frac{c \cdot s_R}{2}$ away from $\mathbb{E}[\mu]$, as Figure 1 shows, enabling concentration argument. Otherwise, bounding the probability of μ_i appears outside the accept region is hard without additional assumptions on $P(\mu)$.*

Lemma 6 suggests that the probability of filtering out a benign gradients decreases at a rate of $\mathcal{O}(\frac{1}{c^2})$. The following lemma further shows the probability of violating the assumed condition $c \geq 2 \cdot \frac{\|\mathbb{E}[\mu]-\bar{\mu}\|}{s_R}$ decreases at a rate of $\mathcal{O}(\frac{1}{N_R^2})$.

Lemma 8. *With Assumptions 2 and 5, for a fixed accept radius $c \cdot s_R$, with probability at most $\frac{4 \cdot \mathrm{Var}[\mu]^2}{N_R^2 \cdot c^2 \cdot s_R^2}$, we have $c \leq 2 \cdot \frac{\|\mathbb{E}[\mu]-\bar{\mu}\|}{s_R}$.*

The following theorem combines and extends the result on expected gradients to estimated gradients.

Theorem 9. *Under Assumptions 2 and 3, with probability at least $\frac{1}{(2 \cdot \sigma^+ \cdot \sqrt{2\pi})^d} \cdot (1 - \frac{4 \cdot \mathrm{Var}[\mu]^2}{c^2 \cdot s_R^2}) \cdot (1 - \frac{4 \cdot \mathrm{Var}[\mu]^2}{N_R^2 \cdot c^2 \cdot s_R^2})$, we have $\|g_i - m_R\| \leq c \cdot s_R$.*

Theorem 9 shows that the risk of filtering out a benign gradient decreases quickly w.r.t. c and N_R, enabling our strategy of using a small number of reference clients and a conservative c.

5.2 Re-weighting (Stage 2)

Suppose the adversary adopts the Mimic-Shift attack and bypasses the filtering defense. We would like to figure out the probability of assigning a higher scalar projection to the malicious gradient g' than a benign gradient $g_i, i \in \{1, ..., N\}$.

Theorem 10. *Suppose all the gradients pass the filtering phase. Let the aggregated gradient be $\bar{g}^* = w \cdot \bar{g} + w' \cdot g'$, where $(w, w') = \left(\frac{\sum_{i=1}^{N} n_i}{\sum_{i=1}^{N+N'} n_i}, \frac{\sum_{i=N+1}^{N+N'} n_i}{\sum_{i=1}^{N+N'} n_i} \right)$. Let θ be the angle between $\bar{g}$ and*

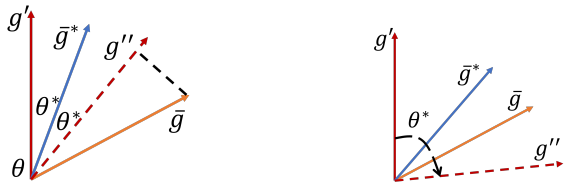

(a) $2 \cdot \theta^* \leq \theta$ case. (b) General case.

Figure 2: Two cases where the adversary mislead the aggregated gradient $\bar{g}^*$ by different degree. $\bar{g}$ is benign. g'' is a mirror of malicious g' w.r.t. $\bar{g}^*$, along which the scalar projection equals to s'.

g', θ^* be the angle between $\bar{g}^*$ and g'. Assume $\frac{w}{w'} \leq \frac{\|g'\| - \cos\frac{\theta}{2} \cdot \|\bar{g}\|}{\|\bar{g}\| - \cos\frac{\theta}{2} \cdot \|g'\|}$ such that $\theta^* \leq \theta - \theta^*$. Then, under Assumptions 1- 5, let $\gamma^-_{\theta^*} = \|\gamma^-\| \cdot \tanh(\theta - 2 \cdot \theta^*)$, with probability at least $\frac{1}{(2 \cdot \sigma^+ \cdot \sqrt{2\pi})^d} \cdot \int_{\alpha=0-}^{\gamma^-_{\theta^*}} \left(1 - \frac{\mathrm{Var}[\mu]}{\alpha^2}\right) \cdot \left(1 - \frac{\mathrm{Var}[\mu]}{(\gamma^-_{\theta^*} - \alpha)^2}\right) d\alpha$, we have $s' \geq s_i, \forall i \in \{1, ..., N\}$.

Theorem 10 suggests that if $2 \cdot \theta^* \leq \theta$, the probability of down-weighting malicious gradients more than benign gradients (i.e., $s' > s_i$) increases as the adversary owns more clients and samples in a system (i.e. $w' \uparrow$). The main idea is: the minimum amount of deviation between g_i and $\bar{g}$ for having $s_i > s'$ increases as w' increases because $w' \uparrow \rightsquigarrow \theta^* \downarrow$. This specific deviation is shown in Figure 2a as the dark dash line with length at least $\|\gamma^-\| \cdot \tanh(\theta - 2 \cdot \theta^*)$. Then, applying concentration arguments yields the result.

5.2.1 Additional Discussion

Theorem 10 only deals with the case where $\bar{g}^*$ has a smaller angle with g' than $\bar{g}$. However, in practice, we find that our method also achieves a decent accuracy even the condition $2 \cdot \theta^* \leq \theta$ does not hold. To gain some insight, suppose there is a probability density function f of benign gradients. Then, the probability of having $s_i > s', \forall i \in \{1, ..., N\}$ equals the integral of f over a cone, which is defined by spinning g' around $\bar{g}^*$ as Figure 2b shows. In a federated scenario, the estimated g_i concentrates around its own μ_i, which is not necessarily close to $\bar{g}$ or $\bar{\mu}$, resulting in a small integral of f over the aforementioned cone.

5.3 Convergence Analysis

So far, our analysis has focused on the robustness of one update. The following extends the single step analysis to a convergence analysis. Before showing the theorem, we present a lemma that quantifies the impact of false-positive filtering.

Lemma 11. *Suppose $\mathcal{F} : N \times R^d \to N \times \{0, 1\}$ is a filtering function, let mask $M = \mathcal{F}(g_1, ..., g_N)$, $N'_F = 1 - \|M\|_1$, $\hat{g} = \frac{1}{\|M\|_1} \cdot \sum_{i=1}^{N} M_i \cdot g_i$, and $\delta = \hat{g} - \bar{g}$. Then, with Assumption 5, we have $\|\delta\| \leq \frac{2 \cdot N'_F}{N} \cdot \gamma^+$.*

In the following theorem, we use assumed conditions to ease the reading. Later , we shall connect the assumed conditions to Theorems 9 and 10 and further support the assumed conditions with empirical results in Appendix C.

Theorem 12. *Suppose the malicious gradient g'_t is filtered out with probability 0, $\forall t \in \{1, ..., T\}$, and down-weighted by $s'_t \geq 1$. Assume at most N'_F benign gradient are filtered out at each iteration. Define an aggregated gradient $\bar{g}^*_t = w \cdot \hat{g}_t + w' \cdot \frac{g'_t}{s'_t} = w \cdot (\bar{\mu}_t + \delta_t + \epsilon_t) + w' \cdot \frac{g'_t}{s'_t}$, where $\hat{g}_t$ and δ_t follow the definitions in Lemma 11, $\epsilon_t \sim \frac{1}{N} \cdot \sum_{i=1}^{N} \mathcal{N}(0, \sigma_{t,i})$ as Assumption 2 shows. Let $\zeta \in Z$ be the model parameter, ζ^* be the optimum, and $\bar{\zeta} = \frac{1}{T} \sum_{t=1}^{T} \zeta_t$. Assume $\sup_{\zeta \in Z} \|\zeta\| \leq D$ and $F : Z \to \mathbb{R}$ is convex. Let $C = w \cdot \frac{2 \cdot N'_F}{N} \cdot \gamma^{+2} + 2 \cdot w \cdot \gamma^{+2} + w' \cdot \gamma^{+2}$, $C' = 2 \cdot w \cdot C + C^2 + w \cdot \gamma^+$, and $\eta_t = \frac{D}{\sqrt{T} \cdot C'}$, under Assumptions 2 and 5, we have:*

$$\mathbb{E}[F(\bar{\zeta})] - F(\zeta^*) \leq \frac{(4 \cdot C' + 1) \cdot D}{2 \cdot w \cdot \sqrt{T}} + \frac{2 \cdot D}{T} \cdot \sum_{t=1}^{T} \left(\|\delta_t\| + \frac{w'}{w \cdot s'_t} \cdot \|g'_t\| + \|\epsilon_t\| \right). \tag{6}$$

The convergence analysis shows that our method converges to a neighborhood around the optimum, whose size shrinks with fewer false-positive filtering (Theorem 9) and more down-weighting (tuning k and τ in Algorithm 2) with higher probability (Theorem 10) on the malicious gradients. Converging to a neighborhood is common in previous noisy gradient descent studies (Wang et al., 2021; He et al., 2022a). Our result also suggests scaling up the learning rate as the adversary owns more clients. In practice, this scaling is handled by our re-weighting phase where the benign gradients are down-weighted by scalars less than 1.

6 EXPERIMENTS

We first compare the Mimic-Shift attack with the Mimic attack, showing that Mimic-Shift is more effective and the improved effectiveness remains with a non-omniscient adversary (Mimic-Shift-Par). Then, we evaluate our defense strategy against the Mimic-Shift attack where our strategy outperforms strong baselines.

Additional Results Appendix C provides more results. We evaluate our defense via a non-omniscient Mimic-Shift-Par attack, an improved Mimic-Shift-Var attack as well as other standard attacks (e.g., Gaussian and sign-flipping). There are also additional experiment with fewer clients and various attack strengths, plots of the re-weighting vector s as well as convergence, and studies on defense hyper-parameters.

6.1 SETUP

We use three datasets, FEMNIST (FM) (Caldas et al., 2018), CelebA (CA) (Liu et al., 2015), and Shakespeare (SS) (McMahan et al., 2017), with realistic non-i.i.d. partitions (Caldas et al., 2018) implemented in the FedML library (He et al., 2020). The number of benign clients ranges from 143 to 500. We select 2 reference clients and 28 other benign clients at each round. The number of adversarial clients is adjusted accordingly. We report the detailed setup in Appendix B, including various hyper-parameters.

We employ seven baselines, including federated averaging (FedAvg) (McMahan et al., 2017), federated averaging with reference clients (Ref), coordinate-wise median (CM) (Yin et al., 2018), FLTrust (Cao et al., 2021), Krum (Blanchard et al., 2017), Krum with bucketing (Krum-B) (Karimireddy et al., 2022), self-centered clipping with reference clients (CClip-R) (Karimireddy et al., 2022; He et al., 2022b), Zeno$'$ (Xie et al., 2019b), and FLTrust (Appendix C.1) (Cao et al., 2021). Appendix B lists the details of these baselines. The "Oracle" aggregator operates with benign gradients and serves as a reference. Five attacks are considered in our experiments, including Mimic-Shift-Var, particularly designed as a strong attack for our proposed defense.

Gaussian Draw a random update g_i' from an isotropic Gaussian distribution $\mathcal{N}(0, 200)$.

Sign-flipping Flip the sign of the estimated gradient $g_i' = -g_i$ and report g_i' to the server.

Mimic-Shift Report $g' = \bar{g}_R + (\bar{g}_R - \bar{g})$ to the server, as is shown in Section 3.1.

Mimic-Shift-Par Randomly eavesdrop 20% clients per round and draw two clients as reference.

Mimic-Shift-Var Mirror the local update using $\bar{g}_R$ and report $g_i' = \bar{g}_R + (\bar{g}_R - \bar{g}_i)$ to the server.

6.2 MIMIC-TYPE ATTACK COMPARISON

Table 1 shows the accuracy of FedAvg aggregator under Mimic and Mimic-Shift attack. Here, the adversary owns 80% of the system, and the Mimic adversary mimics the first client in the system. Mimic-Shift attack constantly outperforms Mimic and is 116% more effective on average. Such advantages are preserved under a non-omniscient adversary.

Table 1: Accuracy of FedAvg Aggregator under Attack with 80% Adversary

Attack Method	FEMNIST	CelebA	Shakespeare	Avg. Decrease
No Attack	.861 $\pm$ .001 (.000$\downarrow$)	.869 $\pm$ .001 (.000$\downarrow$)	.364 $\pm$ .001 (.000$\downarrow$)	.000$\downarrow$
Mimic	.693 $\pm$ .001 (.168$\downarrow$)	.816 $\pm$ .001 (.053$\downarrow$)	.345 $\pm$ .001 (.019$\downarrow$)	.078$\downarrow$
Mimic-Shift	.621 $\pm$ .001 (.240$\downarrow$)	.797 $\pm$ .001 (.072$\downarrow$)	.169 $\pm$ .001 (.195$\downarrow$)	.169$\downarrow$
Mimic-Shift-Par	.663 $\pm$ .001 (.198$\downarrow$)	.812 $\pm$ .001 (.054$\downarrow$)	.182 $\pm$ .001 (.182$\downarrow$)	.145$\downarrow$

Note: Variance is rounded up.

6.3 Defense against Mimic-Shift Attack

This experiment considers three settings where the adversary owns 0% - 80% of a system. The hyper-parameters of each aggregator are selected based on the 80% adversary setting and directly applied to the other settings. Table 2 shows the accuracy of our strategy and baselines under the Mimic-Shift attack.

Under a majority adversary setting, our method outperforms all the baselines by a large margin. The reason is that the median-based (CM) method picks the malicious gradient once the adversary becomes the majority. Clustering-based (Krum and Krum-B) methods suffers from a similar issue. Other reference client-assisted distance-based re-weighting strategy (CClip-R) and filtering strategy (Zeno$'$) is not effective because Mimic-Shift carefully calibrates the malicious gradients so that they are as close to the reference gradients as the benign gradients. Using only reference clients (Ref) outperforms existing robust aggregators but suffers from low client utilization.

We also find that our proposed defense yields the best accuracy under a minority adversary setting, as discussed in Section 5.2.1. Under a no adversary setting, our strategy weights the benign gradients nearly uniformly without interfering with the training. Our method occasionally outperforms the oracle. We hypothesize that the improved results can come from the up-weighting of the under-represented clients (Li et al., 2020), whose influence score is small.

Table 2: Accuracy of Aggregators Under Mimic-Shift Attack

Adv %	Data	Oracle	Ours	FedAvg	Ref	CM	Krum	Krum-B	CClip-R	Zeno$'$
80%	FM	.861	**.840**	.621	.761	.535	.554	.525	.562	.527
	CA	.870	**.877**	.797	.820	.782	.787	.865	.792	.805
	SS	.364	**.360**	.169	.236	.189	.186	.183	.160	.194
	Avg	.698	**.692**	.529	.606	.502	.509	.525	.505	.509
40%	FM	.861	**.871**	.797	.761	.815	.537	.603	.583	.533
	CA	.870	**.893**	.862	.820	.857	.836	.858	.839	.845
	SS	.364	**.340**	.291	.236	.210	.089	.202	.243	.191
	Avg	.698	**.701**	.650	.606	.627	.487	.554	.555	.523
00%	FM	.861	**.864**	.861	.761	.801	.727	.842	.760	.751
	CA	.870	**.879**	.870	.820	.865	.856	.863	.862	.860
	SS	.364	.357	**.364**	.236	.217	.189	.307	.266	.258
	Avg	.698	**.700**	.698	.606	.628	.591	.671	.629	.623

Note: The numbers are average accuracy over three runs.

7 Conclusion and Future Work

This paper shows two methods for improving the adversarial robustness of federated learning under a majority adversary regime. Empirical results in various settings and against a broad class of attacks demonstrate the proposed methods' effectiveness. Additional theoretical analysis is conducted under the Mimic-Shift attack regime, showing conditions under which the proposed method helps. Further exploring the limitations of learning with majority adversaries is a good next step.

REFERENCES

AppleSupport. Secure enclave. https://support.apple.com/guide/security/secure-enclave-sec59b0b31ff/web.

Jeremy Bernstein, Jiawei Zhao, Kamyar Azizzadenesheli, and Anima Anandkumar. signSGD with majority vote is communication efficient and fault tolerant. In *International Conference on Learning Representations*, 2019. URL https://openreview.net/forum?id=BJxhijAcY7.

Peva Blanchard, El Mahdi El Mhamdi, Rachid Guerraoui, and Julien Stainer. Machine learning with adversaries: Byzantine tolerant gradient descent. In I. Guyon, U. Von Luxburg, S. Bengio, H. Wallach, R. Fergus, S. Vishwanathan, and R. Garnett (eds.), *Advances in Neural Information Processing Systems*, volume 30. Curran Associates, Inc., 2017. URL https://proceedings.neurips.cc/paper/2017/file/f4b9ec30ad9f68f89b29639786cb62ef-Paper.pdf.

Adrien Bonguet and Martine Bellaïche. A survey of denial-of-service and distributed denial of service attacks and defenses in cloud computing. *Future Internet*, 9:43, 2017.

Sebastian Caldas, Peter Wu, Tian Li, Jakub Konečný, H. Brendan McMahan, Virginia Smith, and Ameet Talwalkar. LEAF: A benchmark for federated settings. *CoRR*, abs/1812.01097, 2018. URL http://arxiv.org/abs/1812.01097.

Xiaoyu Cao, Minghong Fang, Jia Liu, and Neil Zhenqiang Gong. Fltrust: Byzantine-robust federated learning via trust bootstrapping. *ArXiv*, abs/2012.13995, 2021.

Lingjiao Chen, Hongyi Wang, Zachary Charles, and Dimitris Papailiopoulos. DRACO: Byzantine-resilient distributed training via redundant gradients. In Jennifer Dy and Andreas Krause (eds.), *Proceedings of the 35th International Conference on Machine Learning*, volume 80 of *Proceedings of Machine Learning Research*, pp. 903–912. PMLR, 10–15 Jul 2018. URL https://proceedings.mlr.press/v80/chen18l.html.

Deepesh Data and Suhas Diggavi. Byzantine-resilient high-dimensional sgd with local iterations on heterogeneous data. In Marina Meila and Tong Zhang (eds.), *Proceedings of the 38th International Conference on Machine Learning*, volume 139 of *Proceedings of Machine Learning Research*, pp. 2478–2488. PMLR, 18–24 Jul 2021. URL https://proceedings.mlr.press/v139/data21a.html.

Minghong Fang, Xiaoyu Cao, Jinyuan Jia, and Neil Gong. Local model poisoning attacks to {Byzantine-Robust} federated learning. In *29th USENIX Security Symposium (USENIX Security 20)*, pp. 1605–1622, 2020.

James Gleeson, Sreekumar Rajan, and Vandana Saini. Gpu encrypt: Aes encryption on mobile devices. 2014.

GoogleBlog. Pixel 6: Setting a new standard for mobile security. https://security.googleblog.com/2021/10/pixel-6-setting-new-standard-for-mobile.html. Published: October 27, 2021.

Chaoyang He, Songze Li, Jinhyun So, Mi Zhang, Hongyi Wang, Xiaoyang Wang, Praneeth Vepakomma, Abhishek Singh, Hang Qiu, Li Shen, Peilin Zhao, Yan Kang, Yang Liu, Ramesh Raskar, Qiang Yang, Murali Annavaram, and Salman Avestimehr. Fedml: A research library and benchmark for federated machine learning. *CoRR*, abs/2007.13518, 2020. URL https://arxiv.org/abs/2007.13518.

Lie He, Sai Praneeth Karimireddy, and Martin Jaggi. Byzantine-robust decentralized learning via self-centered clipping. *CoRR*, abs/2202.01545, 2022a. URL https://arxiv.org/abs/2202.01545.

Lie He, Sai Praneeth Karimireddy, and Martin Jaggi. Byzantine-robust decentralized learning via self-centered clipping. *ArXiv*, abs/2202.01545, 2022b.

Peter Kairouz, H Brendan McMahan, Brendan Avent, Aurélien Bellet, Mehdi Bennis, Arjun Nitin Bhagoji, Kallista Bonawitz, Zachary Charles, Graham Cormode, Rachel Cummings, et al. Advances and open problems in federated learning. *Foundations and Trends® in Machine Learning*, 14(1–2):1–210, 2021.

Sai Praneeth Karimireddy, Lie He, and Martin Jaggi. Learning from history for byzantine robust optimization. In Marina Meila and Tong Zhang (eds.), *Proceedings of the 38th International Conference on Machine Learning*, volume 139 of *Proceedings of Machine Learning Research*, pp. 5311–5319. PMLR, 18–24 Jul 2021a. URL https://proceedings.mlr.press/v139/karimireddy21a.html.

Sai Praneeth Karimireddy, Lie He, and Martin Jaggi. Learning from history for byzantine robust optimization. In Marina Meila and Tong Zhang (eds.), *Proceedings of the 38th International Conference on Machine Learning*, volume 139 of *Proceedings of Machine Learning Research*, pp. 5311–5319. PMLR, 18–24 Jul 2021b. URL https://proceedings.mlr.press/v139/karimireddy21a.html.

Sai Praneeth Karimireddy, Lie He, and Martin Jaggi. Byzantine-robust learning on heterogeneous datasets via bucketing. In *International Conference on Learning Representations*, 2022. URL https://openreview.net/forum?id=jXKKDEi5vJt.

Tian Li, Maziar Sanjabi, Ahmad Beirami, and Virginia Smith. Fair resource allocation in federated learning. In *International Conference on Learning Representations*, 2020. URL https://openreview.net/forum?id=ByexElSYDr.

Tian Li, Shengyuan Hu, Ahmad Beirami, and Virginia Smith. Ditto: Fair and robust federated learning through personalization. In Marina Meila and Tong Zhang (eds.), *Proceedings of the 38th International Conference on Machine Learning*, volume 139 of *Proceedings of Machine Learning Research*, pp. 6357–6368. PMLR, 18–24 Jul 2021. URL https://proceedings.mlr.press/v139/li21h.html.

Ziwei Liu, Ping Luo, Xiaogang Wang, and Xiaoou Tang. Deep learning face attributes in the wild. In *Proceedings of International Conference on Computer Vision (ICCV)*, December 2015.

Brendan McMahan, Eider Moore, Daniel Ramage, Seth Hampson, and Blaise Aguera y Arcas. Communication-Efficient Learning of Deep Networks from Decentralized Data. In Aarti Singh and Jerry Zhu (eds.), *Proceedings of the 20th International Conference on Artificial Intelligence and Statistics*, volume 54 of *Proceedings of Machine Learning Research*, pp. 1273–1282. PMLR, 20–22 Apr 2017. URL https://proceedings.mlr.press/v54/mcmahan17a.html.

Fan Mo, Hamed Haddadi, Kleomenis Katevas, Eduard Marin, Diego Perino, and Nicolas Kourtellis. Ppfl: Privacy-preserving federated learning with trusted execution environments. In *Proceedings of the 19th Annual International Conference on Mobile Systems, Applications, and Services*, MobiSys '21, pp. 94–108, New York, NY, USA, 2021. Association for Computing Machinery. ISBN 9781450384438. doi: 10.1145/3458864.3466628. URL https://doi.org/10.1145/3458864.3466628.

Sandro Pinto and Nuno Santos. Demystifying arm trustzone: A comprehensive survey. *ACM Comput. Surv.*, 51(6), jan 2019. ISSN 0360-0300. doi: 10.1145/3291047. URL https://doi.org/10.1145/3291047.

Shashank Rajput, Hongyi Wang, Zachary Charles, and Dimitris Papailiopoulos. Detox: A redundancy-based framework for faster and more robust gradient aggregation. In H. Wallach, H. Larochelle, A. Beygelzimer, F. d'Alché-Buc, E. Fox, and R. Garnett (eds.), *Advances in Neural Information Processing Systems*, volume 32. Curran Associates, Inc., 2019a. URL https://proceedings.neurips.cc/paper/2019/file/415185ea244ea2b2bedeb0449b926802-Paper.pdf.

Shashank Rajput, Hongyi Wang, Zachary Charles, and Dimitris Papailiopoulos. Detox: A redundancy-based framework for faster and more robust gradient aggregation. In H. Wallach, H. Larochelle, A. Beygelzimer, F. d'Alché-Buc, E. Fox, and R. Garnett

(eds.), *Advances in Neural Information Processing Systems*, volume 32. Curran Associates, Inc., 2019b. URL https://proceedings.neurips.cc/paper/2019/file/415185ea244ea2b2bedeb0449b926802-Paper.pdf.

Max Ryabinin and Anton Gusev. Towards crowdsourced training of large neural networks using decentralized mixture-of-experts. In H. Larochelle, M. Ranzato, R. Hadsell, M.F. Balcan, and H. Lin (eds.), *Advances in Neural Information Processing Systems*, volume 33, pp. 3659–3672. Curran Associates, Inc., 2020. URL https://proceedings.neurips.cc/paper/2020/file/25ddc0f8c9d3e22e03d3076f98d83cb2-Paper.pdf.

SamsungDeveloper. Samsung teegris. https://developer.samsung.com/teegris/overview.html.

Virat Shejwalkar, Amir Houmansadr, Peter Kairouz, and Daniel Ramage. Back to the drawing board: A critical evaluation of poisoning attacks on federated learning. *ArXiv*, abs/2108.10241, 2021.

Stephen M. Specht and Ruby B. Lee. Taxonomies of distributed denial of service networks, attacks, tools, and countermeasures. 2003.

Jacob Steinhardt, Pang Wei Koh, and Percy Liang. Certified defenses for data poisoning attacks. In *Proceedings of the 31st International Conference on Neural Information Processing Systems*, NIPS'17, pp. 3520–3532, Red Hook, NY, USA, 2017. Curran Associates Inc. ISBN 9781510860964.

Hongyi Wang, Kartik Sreenivasan, Shashank Rajput, Harit Vishwakarma, Saurabh Agarwal, Jyyong Sohn, Kangwook Lee, and Dimitris Papailiopoulos. Attack of the tails: Yes, you really can backdoor federated learning. In H. Larochelle, M. Ranzato, R. Hadsell, M.F. Balcan, and H. Lin (eds.), *Advances in Neural Information Processing Systems*, volume 33, pp. 16070–16084. Curran Associates, Inc., 2020. URL https://proceedings.neurips.cc/paper/2020/file/b8ffa41d4e492f0fad2f13e29e1762eb-Paper.pdf.

Yunjuan Wang, Poorya Mianjy, and Raman Arora. Robust learning for data poisoning attacks. In Marina Meila and Tong Zhang (eds.), *Proceedings of the 38th International Conference on Machine Learning*, volume 139 of *Proceedings of Machine Learning Research*, pp. 10859–10869. PMLR, 18–24 Jul 2021. URL https://proceedings.mlr.press/v139/wang21r.html.

Chulin Xie, Minghao Chen, Pin-Yu Chen, and Bo Li. Crfl: Certifiably robust federated learning against backdoor attacks. In Marina Meila and Tong Zhang (eds.), *Proceedings of the 38th International Conference on Machine Learning*, volume 139 of *Proceedings of Machine Learning Research*, pp. 11372–11382. PMLR, 18–24 Jul 2021. URL https://proceedings.mlr.press/v139/xie21a.html.

Cong Xie, Oluwasanmi Koyejo, and Indranil Gupta. Fall of empires: Breaking byzantine-tolerant SGD by inner product manipulation. In Amir Globerson and Ricardo Silva (eds.), *Proceedings of the Thirty-Fifth Conference on Uncertainty in Artificial Intelligence, UAI 2019, Tel Aviv, Israel, July 22-25, 2019*, volume 115 of *Proceedings of Machine Learning Research*, pp. 261–270. AUAI Press, 2019a. URL http://proceedings.mlr.press/v115/xie20a.html.

Cong Xie, Sanmi Koyejo, and Indranil Gupta. Zeno: Distributed stochastic gradient descent with suspicion-based fault-tolerance. In Kamalika Chaudhuri and Ruslan Salakhutdinov (eds.), *Proceedings of the 36th International Conference on Machine Learning*, volume 97 of *Proceedings of Machine Learning Research*, pp. 6893–6901. PMLR, 09–15 Jun 2019b. URL https://proceedings.mlr.press/v97/xie19b.html.

Cong Xie, Sanmi Koyejo, and Indranil Gupta. Zeno++: Robust fully asynchronous SGD. In Hal Daumé III and Aarti Singh (eds.), *Proceedings of the 37th International Conference on Machine Learning*, volume 119 of *Proceedings of Machine Learning Research*, pp. 10495–10503. PMLR, 13–18 Jul 2020. URL https://proceedings.mlr.press/v119/xie20c.html.

Dong Yin, Yudong Chen, Ramchandran Kannan, and Peter Bartlett. Byzantine-robust distributed learning: Towards optimal statistical rates. In Jennifer Dy and Andreas Krause (eds.), *Proceedings of the 35th International Conference on Machine Learning*, volume 80 of *Proceedings of Machine Learning Research*, pp. 5650–5659. PMLR, 10–15 Jul 2018. URL https://proceedings.mlr.press/v80/yin18a.html.

A PROOFS

A.1 FILTERING (STAGE 1)

Lemma 6. *Suppose there are N_R reference clients among N clients, and the sample variance of gradients is s_R, under Assumption 2, let $c \geq 2 \cdot \frac{\|\mathbb{E}[\mu]-\bar{\mu}\|}{s^R}$. Then, for any $i \in [1, ..., N]$, , with probability at most $\frac{4 \cdot \mathrm{Var}[\mu]^2}{c^2 \cdot s_R^2}$, we have $\|\mu_i - \bar{\mu}_R\| \geq c \cdot s_R$, where $\bar{\mu}_R = \sum_{i=1}^{R} \frac{1}{N_R} \cdot \mu_{R_i}$.*

Proof. Since $c \geq 2 \cdot \frac{\|\mathbb{E}[\mu]-\bar{\mu}\|}{s_R}$, we have:

$$\mathbb{P}\Big[\|\mu_i - \bar{\mu}_R\| \geq c \cdot s_R\Big] \leq \mathbb{P}\Big[\|\mu_i - \mathbb{E}[\mu]\| \geq \frac{c \cdot s_R}{2}\Big] \tag{7}$$

With Chebyshev's inequality, we have:

$$\mathbb{P}\Big[\|\mu_i - \mathbb{E}[\mu]\| \geq \frac{c \cdot s_R}{2}\Big] \leq \frac{4 \cdot \mathrm{Var}[\mu]^2}{c^2 \cdot s_R^2}. \tag{8}$$

□

Lemma 8. *With Assumptions 2 and 5, for a fixed accept radius $c \cdot s_R$, with probability at most $\frac{4 \cdot \mathrm{Var}[\mu]^2}{N_R^2 \cdot c^2 \cdot s_R^2}$, we have $c \leq 2 \cdot \frac{\|\mathbb{E}[\mu]-\bar{\mu}\|}{s_R}$.*

Proof. With Chebyshev's inequality, we have:

$$\mathbb{P}\Big[\|\mathbb{E}[\mu] - \bar{\mu}\| \geq \frac{c \cdot s_R}{2}\Big] \leq \frac{4 \cdot \mathrm{Var}[\bar{\mu}]^2}{c^2 \cdot s_R^2} = \frac{4 \cdot \mathrm{Var}[\mu]^2}{N_R^2 \cdot c^2 \cdot s_R^2} \tag{9}$$

□

Theorem 9. *Under Assumptions 2 and 3, with probability at least $\frac{1}{(2 \cdot \sigma^+ \cdot \sqrt{2\pi})^d} \cdot (1 - \frac{4 \cdot \mathrm{Var}[\mu]^2}{c^2 \cdot s_R^2}) \cdot (1 - \frac{4 \cdot \mathrm{Var}[\mu]^2}{N_R^2 \cdot c^2 \cdot s_R^2})$, we have $\|g_i - m_R\| \leq c \cdot s_R$.*

Proof. With Assumption 2, we have $g_i = \mu_i + \epsilon_i$, where $\epsilon_i \sim \mathcal{N}(0, \sigma_i)$.

Let $\bar{\epsilon}_R = \sum_{i=1}^{N_R} \frac{1}{N_R} \cdot \epsilon_{R_i}$, with Assumption 1, we have:

$$\|g_i - m_R\| = \|\mu_i + \epsilon_i - \bar{\mu}_R - \bar{\epsilon}_R\|. \tag{10}$$

Then, we derive a lower bound:

$$\mathbb{P}\Big[\|g_i - m_R\| \leq c \cdot s_R\Big] \geq \mathbb{P}\Big[\|\mu_i - \bar{\mu}_R\| \leq c \cdot s_R\Big] \times \mathbb{P}\Big[\|\epsilon_i - \bar{\epsilon}_R\| = 0\Big] \tag{11}$$

Since $\epsilon_i, \forall i \in [1, ..., N]$ are samples from zero-mean Gaussian distributions, we have:

$$\mathbb{P}\Big[\|\epsilon_i - \bar{\epsilon}_R\| = 0\Big] \geq \frac{1}{\Big(2 \cdot \sigma^+ \cdot \sqrt{2\pi}\Big)^d}. \tag{12}$$

With Lemma 6, we have:

$$\mathbb{P}\Big[\|\mu_i - \bar{\mu}_R\| \leq c \cdot s_R\Big] \geq 1 - \frac{4 \cdot \mathrm{Var}[\mu]^2}{c^2 \cdot s_R^2}. \tag{13}$$

Plugging Equations equation 12 and equation 13 to Equation equation 11, we have: .

$$\mathbb{P}\Big[\|g_i - m_R\| \leq c \cdot s_R\Big] \geq \frac{1}{(2 \cdot \sigma^+ \cdot \sqrt{2\pi})^d} \cdot (1 - \frac{4 \cdot \mathrm{Var}[\mu]^2}{c^2 \cdot s_R^2}) \tag{14}$$

Then, with Lemma 8, with a given c and N_R, we have:

$$\mathbb{P}\Big[c \geq 2 \cdot \frac{\|\mathbb{E}[\mu] - \bar{\mu}\|}{s^R}\Big] = \mathbb{P}\Big[\|\mathbb{E}[\mu] - \bar{\mu}\| \leq \frac{c \cdot s_R}{2}\Big] \geq 1 - \frac{4 \cdot \mathrm{Var}[\mu]^2}{N_R^2 \cdot c^2 \cdot s_R^2} \tag{15}$$

Combining Equations equation 14 and equation 15 completes the proof. □

A.2 RE-WEIGHTING (STAGE 2)

Theorem 10. *Suppose all the gradients pass the filtering phase. Let the aggregated gradient be* $\bar{g}^* = w \cdot \bar{g} + w' \cdot g'$*, where* $(w, w') = (\frac{\sum_{i=1}^{N} n_i}{\sum_{i=1}^{N+N'} n_i}, \frac{\sum_{i=N+1}^{N+N'} n_i}{\sum_{i=1}^{N+N'} n_i})$*. Let* θ *be the angle between* $\bar{g}$ *and* g'*,* θ^* *be the angle between* $\bar{g}^*$ *and* g'*. Assume* $\frac{w}{w'} \leq \frac{\|g'\| - \cos\frac{\theta}{2} \cdot \|\bar{g}\|}{\|\bar{g}\| - \cos\frac{\theta}{2} \cdot \|g'\|}$ *such that* $\theta^* \leq \theta - \theta^*$*. Then, under Assumptions 1- 5, let* $\gamma^-_{\theta^*} = \|\gamma^-\| \cdot \tanh(\theta - 2 \cdot \theta^*)$*, with probability at least* $\frac{1}{(2 \cdot \sigma^+ \cdot \sqrt{2\pi})^d} \cdot \int_{\alpha=0^-}^{\gamma^-_{\theta^*}} \Big(1 - \frac{\mathrm{Var}[\mu]}{\alpha^2}\Big) \cdot \Big(1 - \frac{\mathrm{Var}[\mu]}{(\gamma^-_{\theta^*} - \alpha)^2}\Big) d\alpha$*, we have* $s' \geq s_i, \forall i \in \{1, ..., N\}$*.*

Proof. With $\theta^* \leq \theta - \theta^*$, if $s' \geq s_i$, we have $\|g_i - \bar{g}\| \leq \|\bar{g}\| \cdot \tanh(\theta - 2 \cdot \theta^*)$. With Assumption 2, we have $g_i = \mu_i + \epsilon_i$, where $\epsilon_i \sim \mathcal{N}(0, \sigma_i)$. Let $\bar{\epsilon} = \sum_{i=1}^{N} \frac{1}{N} \cdot \epsilon_i$, with Assumption 1, we have:

$$
\begin{aligned}
&\mathbb{P}\Big[s' \geq s_i\Big] \\
&\quad = \mathbb{P}\Big[\|g_i - \bar{g}\| \leq \|\bar{g}\| \cdot \tanh(\theta - 2 \cdot \theta^*)\Big] \\
&\quad \geq \mathbb{P}\Big[\|g_i - \bar{g}\| \leq \|\gamma^-\| \cdot \tanh(\theta - 2 \cdot \theta^*)\Big] \\
&\quad \geq \mathbb{P}\Big[\|\mu_i - \bar{\mu}\| \leq \|\gamma^-\| \cdot \tanh(\theta - 2 \cdot \theta^*)\Big] \times \mathbb{E}[\|\epsilon_i - \bar{\epsilon}\| \ = 0] \\
&\quad \geq \mathbb{P}\Big[\|\mu_i - \mathbb{E}[\mu]\| + \|\mathbb{E}[\mu] - \bar{\mu}\| \leq \|\gamma^-\| \cdot \tanh(\theta - 2 \cdot \theta^*)\Big] \times \mathbb{E}[\|\epsilon_i - \bar{\epsilon}\| \ = 0]
\end{aligned}
\tag{16}
$$

Introducing an auxiliary variable α, we have:

$$
\begin{aligned}
&\mathbb{P}\Big[\|\mu_i - \mathbb{E}[\mu]\| + \|\mathbb{E}[\mu] - \bar{\mu}\| \leq \|\gamma^-\| \cdot \tanh(\theta - 2 \cdot \theta^*)\Big] \\
&\quad = \mathbb{P}\Big[\|\mu_i - \mathbb{E}[\mu]\| \leq \alpha\Big] \times \mathbb{P}\Big[\|\mathbb{E}[\mu] - \bar{\mu}\| \leq \|\gamma^-\| \cdot \tanh(\theta - 2 \cdot \theta^*) - \alpha\Big]
\end{aligned}
\tag{17}
$$

With Chebyshev's inequality, we have:

$$
\begin{aligned}
&\mathbb{P}\Big[\|\mu_i - \mathbb{E}[\mu]\| \leq \alpha\Big] \geq 1 - \frac{\mathrm{Var}[\mu]}{\alpha^2}, \\
&\mathbb{P}\Big[\|\mathbb{E}[\mu] - \bar{\mu}\| \leq \|\gamma^-\| \cdot \tanh(\theta - 2 \cdot \theta^*) - \alpha\Big] \geq 1 - \frac{\mathrm{Var}[\mu]}{\Big(\|\gamma^-\| \cdot \tanh(\theta - 2 \cdot \theta^*) - \alpha\Big)^2},
\end{aligned}
\tag{18}
$$

With Assumption 2, we have:

$$
\mathbb{E}[\|\epsilon_i - \bar{\epsilon}\| \ = 0] = \frac{N+1}{\sigma^+ \cdot \sqrt{2\pi}} \tag{19}
$$

Under Assumption 5, combine Equations equation 16 - equation 19 and integrate α over $(0, \|\gamma^-\| \cdot \tanh(\theta - 2 \cdot \theta^*)]$:

$$
\begin{aligned}
&\mathbb{P}\Big[s' > s_i\Big] \\
&\quad \geq \frac{N+1}{\sigma^+ \cdot \sqrt{2\pi}} \cdot \int_{\alpha=0^-}^{\|\gamma^-\| \cdot \tanh(\theta - 2 \cdot \theta^*)} \Big(1 - \frac{\mathrm{Var}[\mu]}{\alpha^2}\Big) \cdot \Big(1 - \frac{\mathrm{Var}[\mu]}{\Big(\|\gamma^-\| \cdot \tanh(\theta - 2 \cdot \theta^*) - \alpha\Big)^2}\Big) d\alpha.
\end{aligned}
\tag{20}
$$

□

A.3 CONVERGENCE

Lemma 11. *Suppose $\mathcal{F}: N \times R^d \to N \times \{0,1\}$ is a filtering function, let mask $M = \mathcal{F}(g_1, ..., g_N)$, $N'_F = N - \|M\|_1$, $\hat{g} = \frac{1}{\|M\|_1} \cdot \sum_{i=1}^{N} M_i \cdot g_i$, and $\delta = \hat{g} - \bar{g}$. Then, with Assumption 5, we have $\|\delta\| \leq \frac{2 \cdot N'_F}{N} \cdot \gamma^+$.*

Proof. With Assumption 5, we have:

$$\begin{aligned}
\|\delta\| = \|\hat{g} - \bar{g}\| &= \|\frac{1}{\|M\|_1} \cdot \sum_{i=1}^{N} M_i \cdot g_i - \frac{1}{N} \sum_{i=1}^{N} g_i\| \\
&= \|\frac{1}{\|M\|_1} \cdot \sum_{i=1}^{N} M_i \cdot g_i - \Big(\frac{1}{N} \cdot \sum_{i=1}^{N} M_i \cdot g_i + \frac{1}{N} \cdot \sum_{i=1}^{N} (1 - M_i) \cdot g_i\Big)\| \\
&\leq \|\frac{1}{\|M\|_1} \cdot \sum_{i=1}^{N} M_i \cdot g_i - \frac{1}{N} \cdot \sum_{i=1}^{N} M_i \cdot g_i\| + \|\frac{1}{N} \cdot \sum_{i=1}^{N} (1 - M_i) \cdot g_i\| \\
&= \frac{N - \|M\|_1}{\|M\|_1 \cdot N} \|\sum_{i=1}^{N} M_i \cdot g_i\| + \frac{1}{N} \cdot \|\sum_{i=1}^{N} (1 - M_i) \cdot g_i\| \\
&\leq \frac{N'_F}{N} \gamma^+ + \frac{N'_F}{N} \gamma^+ = \frac{2 \cdot N'_F}{N} \gamma^+
\end{aligned} \tag{21}$$

□

Theorem 12. *Suppose the malicious gradient g'_t is filtered out with probability 0, $\forall t \in \{1, ..., T\}$, and down-weighted by $s'_t \geq 1$. Assume at most N'_F benign gradient are filtered out at each iteration. Define an aggregated gradient $\bar{g}^*_t = w \cdot \hat{g}_t + w' \cdot \frac{g'_t}{s'_t} = w \cdot (\bar{\mu}_t + \delta_t + \epsilon_t) + w' \cdot \frac{g'_t}{s'_t}$, where $\hat{g}_t$ and δ_t follow the definitions in Lemma 11, $\epsilon_t \sim \frac{1}{N} \cdot \sum_{i=1}^{N} \mathcal{N}(0, \sigma_{t,i})$ as Assumption 2 shows. Let $\zeta \in Z$ be the model parameter, ζ^* be the optimum, and $\bar{\zeta} = \frac{1}{T} \sum_{t=1}^{T} \zeta_t$. Assume $\sup_{\zeta \in Z} \|\zeta\| \leq D$ and $F: Z \to \mathbb{R}$ is convex. Let $C = w \cdot \frac{2 \cdot N'_F}{N} \cdot {\gamma^+}^2 + 2 \cdot w \cdot {\gamma^+}^2 + w' \cdot {\gamma^+}^2$, $C' = 2 \cdot w \cdot C + C^2 + w \cdot \gamma^+$, and $\eta_t = \frac{D}{\sqrt{T} \cdot C'}$, under Assumptions 2 and 5, we have:*

$$\mathbb{E}[F(\bar{\zeta})] - F(\zeta^*) \leq \frac{(4 \cdot C' + 1) \cdot D}{2 \cdot w \cdot \sqrt{T}} + \frac{2 \cdot D}{T} \cdot \sum_{t=1}^{T} \Big(\|\delta_t\| + \frac{w'}{w \cdot s'_t} \cdot \|g'_t\| + \|\epsilon_t\|\Big). \tag{22}$$

Proof. With the convexity assumption on F:

$$\begin{aligned}
\mathbb{E}[F(\bar{\zeta})] - F(\zeta^*) &= \mathbb{E}[F(\frac{1}{T} \sum_{t=1}^{T} \zeta_t)] - F(\zeta^*) \\
&\leq \mathbb{E}[\frac{1}{T} \sum_{t=1}^{T} F(\zeta_t)] - F(\zeta^*) \\
&= \frac{1}{T} \sum_{t=1}^{T} [\mathbb{E}[F(\zeta_t)] - F(\zeta^*)] \\
&\leq \frac{1}{T} \sum_{t=1}^{T} \mathbb{E}[\langle \bar{\mu}_t, \zeta_t - \zeta^* \rangle].
\end{aligned} \tag{23}$$

Then, we derive an upper bound of $\mathbb{E}[\langle \bar{\mu}_t, \zeta_t - \zeta^* \rangle]$. With Assumption 2 and Lemma 11, by the definition of $\bar{g}^*_t = w \cdot \hat{g}_t + \frac{w'}{s'_t} \cdot g'_t = w \cdot (\bar{\mu}_t + \delta_t + \epsilon_t) + \frac{w'}{s'_t} \cdot g'_t$, we have:

$$
\begin{aligned}
L_{t+1} :&= \mathbb{E}[\|\zeta_{t+1} - \zeta^*\|^2] \\
&= \mathbb{E}[\|\zeta_t - \eta_t \cdot \bar{g}_t^* - \zeta^*\|^2] \\
&= \mathbb{E}[\|\zeta_t - \zeta^*\|^2] - 2 \cdot \eta_t \cdot \mathbb{E}[\langle \bar{g}_t^*, \zeta_t - \zeta^* \rangle] + \eta_t^2 \cdot \mathbb{E}[\|\bar{g}_t^*\|^2] \\
&= L_t - 2 \cdot \eta_t \cdot \mathbb{E}[\langle w \cdot (\bar{\mu}_t + \delta_t + \epsilon_t) + \frac{w'}{s_t'} \cdot g_t', \zeta_t - \zeta^* \rangle] \\
&\quad + \eta_t^2 \cdot \mathbb{E}[\|w \cdot (\bar{\mu}_t + \delta_t + \epsilon_t) + \frac{w'}{s_t'} \cdot g_t'\|^2] \\
&\leq L_t - 2 \cdot \eta_t \cdot \mathbb{E}[\langle w \cdot \bar{\mu}_t, \zeta_t - \zeta^* \rangle] - 2 \cdot \eta_t \cdot \mathbb{E}[\langle w \cdot (\delta_t + \epsilon_t) + \frac{w'}{s_t'} \cdot g_t', \zeta_t - \zeta^* \rangle] \\
&\quad + \eta_t^2 \cdot \mathbb{E}[\|w \cdot (\bar{\mu}_t + \delta_t + \epsilon_t) + \frac{w'}{s_t'} \cdot g_t'\|^2] \\
&\leq L_t - 2 \cdot \eta_t \cdot \mathbb{E}[\langle w \cdot \bar{\mu}_t, \zeta_t - \zeta^* \rangle] - 2 \cdot \eta_t \cdot \mathbb{E}[\|w \cdot (\delta_t + \epsilon_t) + \frac{w'}{s_t'} \cdot g_t'\| \cdot \|\zeta_t - \zeta^*\|] \\
&\quad + \eta_t^2 \cdot \Big(\mathbb{E}[\|w \cdot \bar{\mu}_t\|^2] + 2 \cdot \langle \mathbb{E}[w \cdot \bar{\mu}_t], w \cdot (\delta_t + \epsilon_t) + \frac{w'}{s_t'} \cdot g_t' \rangle + \|w \cdot (\delta_t + \epsilon_t) + \frac{w'}{s_t'} \cdot g_t'\|^2] \Big) \\
&\leq L_t - 2 \cdot \eta_t \cdot \mathbb{E}[\langle w \cdot \bar{\mu}_t, \zeta_t - \zeta^* \rangle] + 4 \cdot \eta_t \cdot D \cdot \|w \cdot (\delta_t + \epsilon_t) + \frac{w'}{s_t'} \cdot g_t'\| \\
&\quad + \eta_t^2 \cdot \Big(w^2 \cdot {\gamma^+}^2 + 2 \cdot w \cdot \gamma^+ \cdot \|w \cdot (\delta_t + \epsilon_t) + \frac{w'}{s_t'} \cdot g_t'\| + \|w \cdot (\delta_t + \epsilon_t) + \frac{w'}{s_t'} \cdot g_t'\|^2] \Big) \\
&\leq L_t - 2 \cdot w \cdot \eta_t \cdot \mathbb{E}[\langle \bar{\mu}_t, \zeta_t - \zeta^* \rangle] + (4 \cdot \eta_t \cdot D + 2 \cdot w \cdot \eta_t^2 \cdot \gamma^+) \cdot \|w \cdot (\delta_t + \epsilon_t) + \frac{w'}{s_t'} \cdot g_t'\| \\
&\quad + \eta_t^2 \cdot \|w \cdot (\delta_t + \epsilon_t) + \frac{w'}{s_t'} \cdot g_t'\|^2 + w \cdot \eta_t^2 \cdot {\gamma^+}^2.
\end{aligned}
\tag{24}
$$

Move $\mathbb{E}[\langle \bar{\mu}_t, \zeta_t - \zeta^* \rangle]$ to the left-hand-side:

$$
\begin{aligned}
\mathbb{E}[\langle \bar{\mu}_t, \zeta_t - \zeta^* \rangle] \leq \frac{L_t - L_{t+1}}{2 \cdot w \cdot \eta_t} + (\frac{2 \cdot D}{w} + \eta_t \cdot \gamma^+) \cdot \|w \cdot (\delta_t + \epsilon_t) + \frac{w'}{s_t'} \cdot g_t'\| \\
+ \frac{\eta_t}{2 \cdot w} \cdot \|w \cdot (\delta_t + \epsilon_t) + \frac{w'}{s_t'} \cdot g_t'\|^2 + \frac{\eta_t}{2} \cdot \gamma^+.
\end{aligned}
\tag{25}
$$

Average over T iterations:

$$\begin{aligned}
\frac{1}{T}\sum_{t=1}^{T}\mathbb{E}[\langle\bar{\mu}_t,\zeta_t-\zeta^*\rangle] &\leq \sum_{t=1}^{T}\frac{L_t-L_{t+1}}{2\cdot w\cdot\eta_t\cdot T}+\frac{2\cdot D}{w\cdot T}\cdot\sum_{t=1}^{T}\|w\cdot(\delta_t+\epsilon_t)+\frac{w'}{s'_t}\cdot g'_t\| \\
&\quad+\frac{\gamma^+}{T}\cdot\sum_{t=1}^{T}\eta_t\cdot\|w\cdot(\delta_t+\epsilon_t)+\frac{w'}{s'_t}\cdot g'_t\| \\
&\quad+\frac{1}{2\cdot w\cdot T}\cdot\sum_{t=1}^{T}\eta_t\cdot\|w\cdot(\delta_t+\epsilon_t)+\frac{w'}{s'_t}\cdot g'_t\|^2+\frac{\gamma^+}{2\cdot T}\cdot\sum_{t=1}^{T}\eta_t \\
&\leq \sum_{t=1}^{T}\frac{L_t-L_{t+1}}{2\cdot w\cdot\eta_t\cdot T}+\frac{2\cdot D}{T}\cdot\sum_{t=1}^{T}\Big(\|\delta_t\|+\|\epsilon_t\|+\frac{w'}{w\cdot s'_t}\cdot\|g'_t\|\Big) \\
&\quad+\frac{w\cdot\frac{2\cdot N'_F}{N}\cdot{\gamma^+}^2+2\cdot w\cdot{\gamma^+}^2+w'\cdot{\gamma^+}^2}{T}\cdot\sum_{t=1}^{T}\eta_t \\
&\quad+\frac{\sum_{t=1}^{T}\eta_t\cdot(w\cdot\frac{2\cdot N'_F}{N}\cdot{\gamma^+}^2+2\cdot w\cdot{\gamma^+}^2+w'\cdot{\gamma^+}^2)^2}{2\cdot w\cdot T} \\
&\quad+\frac{\gamma^+}{2\cdot T}\cdot\sum_{t=1}^{T}\eta_t.
\end{aligned} \tag{26}$$

To simplify the notation, we use the condition $s'_t \geq 1$ in the second inequality of Equation equation 26 such that $\|\frac{w'}{s'_t}\cdot g'_t\| \leq w'\cdot\gamma^+$. Let $C = w\cdot\frac{2\cdot N'_F}{N}\cdot{\gamma^+}^2+2\cdot w\cdot{\gamma^+}^2+w'\cdot{\gamma^+}^2$, we have:

$$\begin{aligned}
\frac{1}{T}\sum_{t=1}^{T}\mathbb{E}[\langle\bar{\mu}_t,\zeta_t-\zeta^*\rangle] &\leq \sum_{t=1}^{T}\frac{L_t-L_{t+1}}{2\cdot w\cdot\eta_t\cdot T}+\frac{2\cdot D}{T}\cdot\sum_{t=1}^{T}\Big(\|\delta_t\|+\|\epsilon_t\|+\frac{w'}{w\cdot s_t}\cdot\|g'_t\|\Big) \\
&\quad+\frac{C}{T}\cdot\sum_{t=1}^{T}\eta_t+\frac{C^2}{2\cdot w\cdot T}\cdot\sum_{t=1}^{T}\eta_t+\frac{\gamma^+}{2\cdot T}\cdot\sum_{t=1}^{T}\eta_t \\
&\leq \sum_{t=1}^{T}\frac{L_t-L_{t+1}}{2\cdot w\cdot\eta_t\cdot T}+\frac{2\cdot D}{T}\cdot\sum_{t=1}^{T}\Big(\|\delta_t\|+\|\epsilon_t\|+\frac{w'}{w\cdot s_t}\cdot\|g'_t\|\Big) \\
&\quad+\frac{2\cdot w\cdot C+C^2+w\cdot\gamma^+}{2\cdot w\cdot T}\sum_{t=1}^{T}\eta_t.
\end{aligned} \tag{27}$$

Let $C' = 2 \cdot w \cdot C + C^2 + w \cdot \gamma^+$ and $\eta_t = \frac{D}{\sqrt{T} \cdot C'}$, we further have:

$$\begin{aligned}
\frac{1}{T}\sum_{t=1}^{T}\mathbb{E}[\langle \bar{\mu_t}, \zeta_t - \zeta^* \rangle] &\leq \sum_{t=1}^{T}\frac{L_t - L_{t+1}}{2 \cdot w \cdot \eta_t \cdot T} + \frac{2 \cdot D}{T} \cdot \sum_{t=1}^{T}\Big(\|\delta_t\| + \|\epsilon_t\| + \frac{w'}{w \cdot s_t} \cdot \|g_t'\|\Big) \\
&\quad + \frac{C'}{2 \cdot w \cdot T}\sum_{t=1}^{T}\eta_t \\
&\leq \frac{L_1 - L_{t+1}}{2 \cdot w \cdot \frac{D}{\sqrt{T} \cdot C'} \cdot T} + \frac{2 \cdot D}{T} \cdot \sum_{t=1}^{T}\Big(\|\delta_t\| + \|\epsilon_t\| + \frac{w'}{w \cdot s_t} \cdot \|g_t'\|\Big) \\
&\quad + \frac{C'}{2 \cdot w \cdot T}\sum_{t=1}^{T}\frac{D}{\sqrt{T} \cdot C'} \\
&\leq \frac{4 \cdot D^2}{2 \cdot w \cdot \frac{D}{\sqrt{T} \cdot C'} \cdot T} + \frac{D}{2 \cdot w \cdot \sqrt{T}} \\
&\quad + \frac{2 \cdot D}{T} \cdot \sum_{t=1}^{T}\Big(\|\delta_t\| + \|\epsilon_t\| + \frac{w'}{w \cdot s_t} \cdot \|g_t'\|\Big) \\
&\leq \frac{(4 \cdot C' + 1) \cdot D}{2 \cdot w \cdot \sqrt{T}} + \frac{2 \cdot D}{T} \cdot \sum_{t=1}^{T}\Big(\|\delta_t\| + \|\epsilon_t\| + \frac{w'}{w \cdot s_t} \cdot \|g_t'\|\Big).
\end{aligned} \tag{28}$$

Combining Equations equation 23 and equation 28 completes the proof:

$$\mathbb{E}[F(\bar{\zeta})] - F(\zeta^*) \leq \frac{(4 \cdot C' + 1) \cdot D}{2 \cdot w \cdot \sqrt{T}} + \frac{2 \cdot D}{T} \cdot \sum_{t=1}^{T}\Big(\|\delta_t\| + \frac{w'}{w \cdot s_t'} \cdot \|g_t'\| + \|\epsilon_t\|\Big). \tag{29}$$

□

B Experimental Setup

This section details our setup for datasets (B.1), hyper-parameters (B.2), baselines (B.3), and attacks (B.4).

B.1 Datasets, Tasks, Partitions, and Models

FEMNIST The FEMNIST dataset includes images of 62 hand-written characters from different writers, formulating a 62-way image classification task. We consider a natural non-i.i.d. data partition where 205 clients represent 205 writers. The model for the FEMNIST dataset is a convolutional neural network (CNN) with two convolutional layers and two linear layers.

CelebA The CelebA dataset contains face images of celebrities. Here, a binary classification task is predicting whether the celebrity is smiling or not. We adopt a natural non-i.i.d. partition where each client represents a different set of celebrities, with 500 clients in total. We use a CNN with two convolutional layers and two linear layers on the CelebA dataset.

Shakespeare The Shakespeare dataset comprises Shakespeare's plays. We investigate a next-character prediction task and a natural non-i.i.d. partition where each speaking role in the plays is associated with a different client. There are 143 clients in total. The model on Shapespeare dataset is a recurrent neural network (RNN) with one long short-term memory (LSTM) layer and one linear layer.

B.2 Hyper-parameters

Table 3 summarizes the hyper-parameters. The reference clients and other benign clients are sampled separately from disjoint sets of clients using the same sampling rate.

Table 3: Hyper-parameters

Hyper-parameters	FEMNIST	CelebA	Shakespeare
Optimizer	SGD	Adam	SGD
Learning Rate	0.1	0.0001	3.0
Batch Size	20	32	10
Local Epoch	1	1	1
Communication Round	200	100	200
Number of Benign Clients per Round	30	30	30
Number of Reference Clients per Round	2	2	2
c	1.0	3.0	1.0
k	10	10	10
τ	0.6	0.6	0.6

B.3 BASELINES

Coordinate-wise Median (CM) CM aggregator computes the median of the reported gradients $\{g_i \mid i \in \{1, ..., N + N'\}\}$.

Krum Krum aggregator identifies a set of gradients that are close to each other. Specifically, for the i^{th} gradient, Krum assign a score $s_i = \sum_{i \to j} \|g_i - g_j\|$, where $i \to j$ denotes g_j belongs to the $N - 2$ closest gradients to g_i. Then, we select and aggregate the top $0.2 \cdot (N + N')$ gradients with the highest scores, following the Multi-Krum variant (Blanchard et al., 2017).

Krum with Bucketing (Krum-B) Bucketing improves a few existing defenses under a federated learning scenario, including Krum. Here, we first randomly partition the gradients to $\frac{N}{2}$ buckets (Karimireddy et al., 2022). Then, we average the gradients within each bucket and produce a set of bucketed gradients. The bucketed gradients will be subsequently fed into robust aggregators like Krum.

Self-centered Clipping with Reference Users (CClip-R) Self-centered clipping weights each gradient based on its distance to a guess of the true gradient. Here, we let the guess be the aggregated reference gradient $\bar{g}_R^* := \sum_{i=1}^{N_R} \frac{n_{R_i}}{\sum_{i=1}^{N_R} n_{R_i}} g_{R_i}$. With $\bar{g}_R^*$, we compute a score for each g_i: $s_i = \min(1, \frac{10}{\|g_i - \bar{g}_R^*\|})$. The scores are normalized such that the sum equals to N. The CClip-R aggregator follows a aggregation rule: $\bar{g}^* = \bar{g}_R^* + \sum_{i=1}^{N} \frac{n_i}{\sum_{i=1}^{N} n_i} \cdot s_i \cdot (g_i - \bar{g}_R^*)$.

Zeno$'$ Zeno$'$ is a variant of Zeno (Xie et al., 2019b) for federated learning. Instead of evaluating the update from each client on a validation dataset, we compute the inner product of each update with the aggregated reference gradient, which can be considered a first-order approximation of Zeno. Then, we select and aggregate the top $0.2 \cdot (N + N')$ gradients with the highest inner products.

FLTrust FLTrust is similar to Zeno$'$ but uses cosine-similarity between each update and the aggregated reference gradient to weight each client.

B.4 ATTACK SETUP

B.4.1 MIMIC-SHIFT ATTACK

For CM, Krum, Krum-B, and Zeno$'$ aggregators, we adopt N' adversarial client such that $\frac{N'}{N}$ equals the percentage of a system that the adversary owns. Each adversarial client has $\frac{1}{N} \sum_{i=1}^{N} n_i$ samples. For our method and CClip-R, since the re-weighting factor is the same across all the adversarial clients, we use one adversarial client with n' samples, where $\frac{n'}{n' + \sum_{i=1}^{N} n_i}$ equals the percentage of a system that the adversary owns, to speed up the computation.

B.4.2 MIMIC-SHIFT-VAR ATTACK AND SIGN-FLIPPING ATTACK

For these two attacks, we let $N' = N$ and the i^{th} adversarial client has n_i samples, where $\frac{n_i'}{n_i'+n_i}$ equals the percentage of a system that the adversary owns.

B.4.3 GAUSSIAN ATTACK

We adopt N' adversarial client such that $\frac{N'}{N}$ equals the percentage of a system that the adversary owns.. Each adversarial client has $\frac{1}{N}\sum_{i=1}^{N} n_i$ samples.

C EXPERIMENT DETAILS

This section shows additional experimental results, including (1) the accuracy of FLTrust (Cao et al., 2021) (C.1), (2) defense against Mimic-Shift-Par, Mimic-Shift-Var, and standard attacks (C.2, C.3, C.4) (3) the accuracy of our method with weaker adversaries (C.8), (4) the accuracy of our method with fewer clients (C.9), (5) the distribution of the re-weighting factor s under Mimic-Shift and Mimic-Shift-Var attacks (C.10, C.11), (6) convergence plots under the Mimic-Shift attack (C.12), and (7) ablation studies on hyper-parameters c, N_R, and k (C.13, C.14).

C.1 FLTRUST

FLTrust (Cao et al., 2021) uses the cosine similarity between each gradient and the reference gradient to weight the clients. Then, negative similarities are clipped by a ReLU function. Mimic-type attacks do not incur much difference between the malicious and benign gradients, making FLTrust less effective.

Table 4: Accuracy of Aggregators under Mimic-Shift with 80% Adversary

Attack Method	FEMNIST	CelebA	Shakespeare
Ours	.840 $\pm$ .001	.877 $\pm$ .001	.360 $\pm$ .001
FLTrust	.579 $\pm$ .001	.595 $\pm$ .001	.089 $\pm$ .001
FedAvg	.621 $\pm$ .001	.797 $\pm$ .001	.169 $\pm$ .001

Note: Variance is rounded up.

C.2 DEFENSE AGAINST MIMIC-SHIFT-PAR ATTACKS

An Mimic-Shift-Par adversary can intercept the message from 20% clients. Under our setup, the adversary eavesdrops 6 out of 30 clients at each round and select two of them as reference clients. Table 5 summarizes the results.

Table 5: Accuracy of Aggregators under Mimic-Shift-Par with 80% Adversary

Attack Method	FEMNIST	CelebA	Shakespeare
FedAvg	.663 $\pm$ .001	.812 $\pm$ .001	.182 $\pm$ .001
Ours	.833 $\pm$ .001	.860 $\pm$ .001	.348 $\pm$ .001
Ref	.761 $\pm$ .001	.820 $\pm$ .001	.236 $\pm$ .001
Krum	.394 $\pm$ .001	.819 $\pm$ .001	.204 $\pm$ .001
FLTrust	.614 $\pm$ .001	.842 $\pm$ .001	.186 $\pm$ .001

Note: Variance is rounded up.

C.3 DEFENSE AGAINST MIMIC-SHIFT-VAR ATTACK

We further test our strategy with the Mimic-Shift-Var attack, which improves Mimic-Shift by adding variance to the malicious gradients. Table 6 shows the accuracy of our aggregator and two high-accuracy aggregators from Table 2. Although our method is less robust against the Mimic-Shift-Var

attack, only Ref performs on par with ours on one of the datasets. On average, our strategy achieves the lowest accuracy decrease. The re-weighting vector s is plotted in Appendix C.11. Due to hardware limits, we reduce the number of benign client at each round to 13 on CelebA dataset, as is discussed in Appendix B.

Table 6: Accuracy of Aggregators under Mimic-Shift-Var Attack with 80% Adversary

Aggregator	FEMNIST	CelebA	Shakespeare	Avg. Decrease
Oracle	.861 $\pm$ .001 (.000$\downarrow$)	.875 $\pm$ .001 (.000$\downarrow$)	.364 $\pm$ .001 (.000$\downarrow$)	.000$\downarrow$
FedAvg	.621 $\pm$ .001 (.240$\downarrow$)	.859 $\pm$ .001 (.016$\downarrow$)	.169 $\pm$ .001 (.195$\downarrow$)	.150$\downarrow$
Ref	.761 $\pm$ .001 (.100$\downarrow$)	.820 $\pm$ .001 (.055$\downarrow$)	.236 $\pm$ .001 (.128$\downarrow$)	.095$\downarrow$
Ours	.792 $\pm$ .001 (.069$\downarrow$)	.888 $\pm$ .001 (-.013$\downarrow$)	.233 $\pm$ .001 (.131$\downarrow$)	.062$\downarrow$

Note: Variance is rounded up.

C.4 Defense against Standard Attacks

Table 7 shows that un-calibrated attacks like the Gaussian attack and the sign-flipping attack can not pass our filtering phase.

Table 7: Accuracy of Our Strategy under Standard Attacks with 80% Adversary

Attack Method	FEMNIST	CelebA	Shakespeare	Average
No Attack	.864 $\pm$ .001	.876 $\pm$ .001	.364 $\pm$ .001	.705
Gaussian	.859 $\pm$ .001	.871 $\pm$ .001	.357 $\pm$ .001	.698
Sign-flipping	.863 $\pm$ .001	.873 $\pm$ .001	.353 $\pm$ .001	.699

Note: Variance is rounded up.

Table 8 shows the success rate of Gaussian and sign-flipping attacks. The success rate is measured by the percentage of malicious gradients that circumvent our filtering phase across all rounds. For the Gaussian attack, our filtering phase removes all the randomly sampled malicious gradients. For the sign-flipping attack, the malicious gradients occasionally bypass our filtering phase. However, the sporadic malicious gradients are insufficient to decrease the accuracy of the ML model.

Table 8: Success Rate of Standard Attacks with 80% Adversary

Attack	FEMNIST	CelebA	Shakespeare
Gaussian	.000 $\pm$ .000	.000 $\pm$ .000	.000 $\pm$ .000
Sign-flipping	.008 $\pm$ .018	.000 $\pm$ .000	.036 $\pm$ .040

C.5 Defense against Local Model Poisoning Attacks

We evaluate our defense against 80% adversaries that perform local model poisoning attacks (Fang et al., 2020). Table 9 shows that our aggregator is robust and only loses up to 2.7% accuracy compared to the oracle. Specifically, we let malicious updates be the point in the accept region that maximizes the sign-weighted deviation objective (Equation in (Fang et al., 2020)). Note that we need to assume adversaries know the defense parameter c to circumvent the filtering phase. In contrast, our Mimic-Shift attack does not require any knowledge about the defense parameters (i.e., k and c).

C.6 Defense against 20% Adversaries

We conduct additional evaluations of our defense against 20% adversaries with Mimic-Shift attacks. Table 10 shows that our approach remains effective on the FEMNIST and CelebA datasets.

Table 9: Accuracy of Aggregators under Local Model Poisoning with 80% Adversary

Aggregators	FEMNIST	CelebA	Shakespeare
Oracle	.861 $\pm$ .001	.875 $\pm$ .001	.364 $\pm$ .001
FedAvg	.604 $\pm$ .001	.802 $\pm$ .002	.179 $\pm$ .001
Ours	.838 $\pm$ .002	.871 $\pm$ .001	.337 $\pm$ .002

Note: Variance is rounded up.

Table 10: Accuracy of Aggregators under Mimic-Shift with 20% Adversary

Attack Method	FEMNIST	CelebA	Shakespeare
Oracle	.861 $\pm$ .001	.875 $\pm$ .001	.364 $\pm$ .001
FedAvg	.846 $\pm$ .001	.872 $\pm$ .001	.355 $\pm$ .001
Ours	.863 $\pm$ .001	.873 $\pm$ .001	.286 $\pm$ .002

Note: Variance is rounded up.

C.7 Ablation Study of Filtering and Re-weighting Phases

We evaluate the filtering phase against Mimic-Shift attacks and the re-weighting phase against Gaussian attacks. Results in Table 11 showing that a combination of filtering and re-weighting phases are necessary.

Table 11: Accuracy of Aggregators under Attacks with 80% Adversary

Aggregators	Attack	FEMNIST
Filtering Only	Mimic-Shift	.621 $\pm$ .001
Ours	Mimic-Shift	.840 $\pm$ .001
Re-weighting Only	Gaussian	.009 $\pm$ .001
Ours	Gaussian	.859 $\pm$ .001
Re-weighting Only	Sign-flipping	.003 $\pm$ .001
Ours	Sign-flipping	.863 $\pm$ .001

Note: Variance is rounded up.

C.8 Varying Adversarial Ratio and Attack Strength of Mimic-Shift

We test the robustness of our method against weaker attacks, complementing our analysis on strong majority adversary attacks. Specifically, we consider varying the adversarial ratio (the percentage of a adversary in a system) and the shift ratio (a factor on the shift distance of Mimic-Shift attack). For example, if the shift ratio is 0.5, the adversarial clients report $g' = \bar{g}_R + 0.5 \cdot (\bar{g}_R - \bar{g})$ to the server. A 80% adversary is employed for the shift ratio experiment.

From Figure 3, we can see that a minority adversary may decrease the accuracy of our method but only by a small amount ($< 2\%$). Also, the accuracy slightly decreases ($< 3\%$) as the adversarial increases from 40% to 80% or the shift ratio increases. The reason is that we use the same set of hyper-parameters, which down-weights the malicious gradient by the same magnitude. This accuracy decrease can be fixed by increasing k and lowering τ such that the malicious gradients are down-weighted more.

C.9 Defending Fewer Clients

We test the negative impact of false-positive filtering by reducing the total number of clients to 10. We find that false positive filtering happens occasionally, and no client is consistently filtered out.

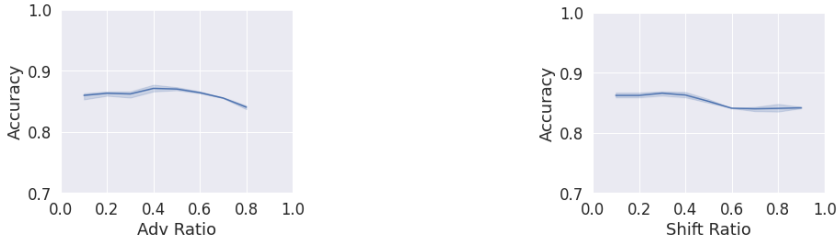

(a) Varying the % of Adversary

(b) Varying % of the Shift Distance

Figure 3: Accuracy of our method with weaker adversaries on FEMNIST dataset.

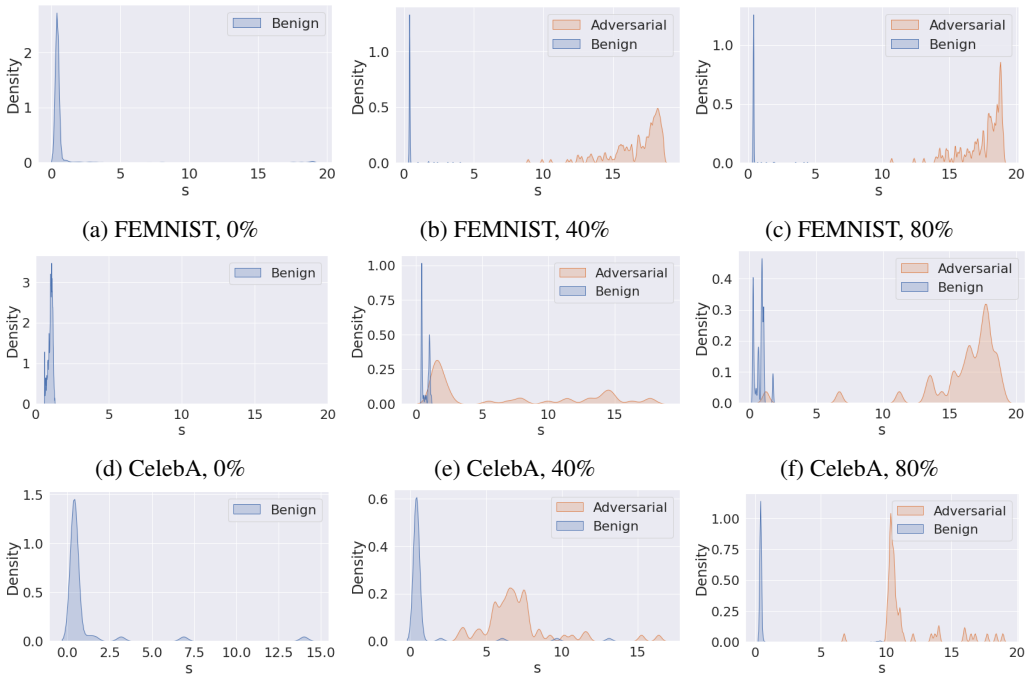

(a) FEMNIST, 0%

(b) FEMNIST, 40%

(c) FEMNIST, 80%

(d) CelebA, 0%

(e) CelebA, 40%

(f) CelebA, 80%

(g) Shakespeare, 0%

(h) Shakespeare, 40%

(i) Shakespeare, 80%

Figure 4: Re-weighting factor s distribution with 0%, 40%, and 80% Mimic-Shift adversaries.

Table 12: Accuracy of Aggregators under Mimic-Shift with 60% Adversary and 10 Clients

Attack Method	FEMNIST	CelebA	Shakespeare
Oracle	.857 $\pm$ .001	.883 $\pm$ .001	.334 $\pm$ .001
FedAvg	.763 $\pm$ .001	.830 $\pm$ .001	.229 $\pm$ .002
Ours	.848 $\pm$ .001	.872 $\pm$ .001	.313 $\pm$ .001

Note: Variance is rounded up.

C.10 Visualizing Re-weighting Vector s under Mimic-Shift Attack

Figure 4 shows the distribution of re-weighting factors s for benign and adversarial clients. The larger the factor, the more the corresponding gradient is down-weighted. The factor for adversarial clients increases and becomes more concentrated as the adversary owns more shares in a system, suggesting that our method is more robust against the majority adversary.

C.11 Visualizing Re-weighting Vector under Mimic-Shift-Var Attack

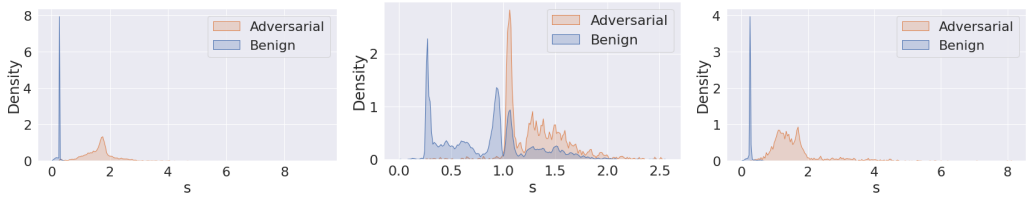

(a) FEMNIST (b) CelebA (c) Shakespeare

Figure 5: Re-weighting factor s distribution under Mimic-Shift-Var attack with 80% adversaries.

Figure 5 shows the distribution of re-weighting factors for benign clients and adversarial clients under Mimic-Shift-Var attack with an 80% adversary. Although the distribution of re-weighting factors for adversarial clients is closer to those of benign clients, compared to the Mimic-Shift attack setting, re-weighting factors for adversarial clients are still larger. The large re-weighting factors down-weight the malicious gradients and reduce the effectiveness of the Mimic-Shift-Var attack.

C.12 Convergence Plots under Mimic-Shift Attack

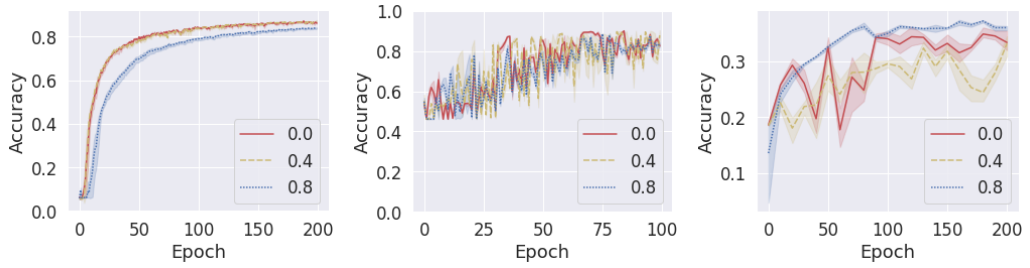

(a) FEMNIST (b) CelebA (c) Shakespeare

Figure 6: Convergence plots of our method with 0%, 40%, and 80% Mimic-Shift adversaries.

Figure 6 shows the convergence plots of our method under Mimic-Shift attack. The convergence rates under three settings, 0% adversary, 40% adversary, and 80% adversary, are similar, supporting our convergence analysis in Section 5.3.

Table 13: False-positive Rate in Filtering Phase with Different c

c	FEMNIST	c	CelebA	Shakespeare
0.2	1.000 $\pm$ .000	1.0	1.000 $\pm$ .000	0.052 $\pm$ .050
0.4	0.911 $\pm$ .067	1.5	0.869 $\pm$ .217	0.058 $\pm$ .069
0.6	0.322 $\pm$ .335	2.0	0.531 $\pm$ .394	0.009 $\pm$ .086
0.8	0.038 $\pm$ .142	2.5	0.113 $\pm$ .199	0.054 $\pm$ .055
1.0	0.018 $\pm$ .096	3.0	0.024 $\pm$ .080	0.052 $\pm$ .054

Table 14: False-positive Rate in Filtering Phase with Different N_R

N_R	FEMNIST	CelebA	Shakespeare
2	.605 $\pm$ .316	.702 $\pm$ .254	.048 $\pm$ .041
4	.432 $\pm$ .264	.076 $\pm$ .098	.038 $\pm$ .040
6	.279 $\pm$ .181	.049 $\pm$ .113	.026 $\pm$ .030

C.13 Impact of c and N_R on False-positive Filtering

This experiment evaluates the false-positive rate in the filtering phase exclusively, without using any adversary. Tables 13 and 14 show that the false-positive rate in the filtering phase decreases fast as the constant c increases and the number of reference users N_R increases, supporting our analysis in Section 5.1. Note that if the false-positive rate is already low (e.g., the experiment on Shakespeare dataset), further increasing c may not be helpful.

C.14 Impact of k on Re-weighting Vector

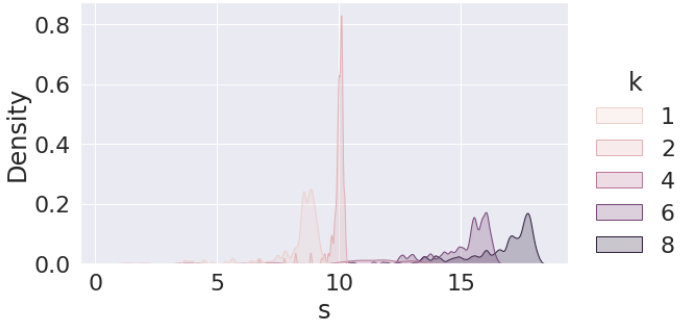

Figure 7: The distribution of re-weighting factor s for malicious gradients.

Figure 7 shows that increasing the hyper-parameter k increases the re-weighting factor s for malicious gradients from an 80% Mimic-Shift adversary.

C.15 Impact of Reference Client Numbers in Mimic-Shift

We evaluate Mimic-Shift attacks with varying numbers of reference clients, showing that our attack is effective with different hyper-parameter configurations. Table 15 demonstrates the effectiveness of the Mimic-Shift attack, which decreases the accuracy from 0.861 to 0.621 - 0.685. Note that Mimic-shift attacks are more effective with fewer reference clients. The reason is that Mimic-Shift mirrors a less biased average update $\bar{g}$ from all sampled clients using a more biased average update $\bar{g}_R$ from reference clients. Here, the more biased an update is, the further away it is from the true expectation. The more biased the average reference update $\bar{g}_R$ is, the more biased the mirroring result is.

Theorem 13 further proves that the probability upper bound of the average reference update $\bar{g}_R$ being more biased than the average update $\bar{g}$ decreases w.r.t. the number of reference clients N_R. Such a result suggests that it is necessary to use fewer reference clients in Mimic-Shift.

Table 15: Accuracies of FedAvg Aggregators under Mimic-Shift Attacks with 80% Adversaries

Number of Reference Clients per Round	FEMNIST
2	.621 $\pm$ .001
4	.653 $\pm$ .001
8	.667 $\pm$ .001
12	.685 $\pm$ .001

Theorem 13. *Under Assumptions 1 - 3, let the average reference gradient* $\bar{g}_R = \sum_{i=1}^{N_R} \frac{1}{N_R} \cdot g_{R_i}$, *where* R_i *indexes reference clients, and the average benign gradient* $\bar{g} = \sum_{i=1}^{N} \frac{1}{N} \cdot g_i$. $\mathbb{E}[\mu]$ *is the expected gradient across benign clients and* α *is an auxiliary variable.* $\diamond$ *denotes* $\int_{\alpha=0}^{\infty} \mathbb{P}\Big[\|\bar{g} - \mathbb{E}[\mu]\| = \alpha\Big] \frac{(\mathrm{Var}[\mu]+\sigma^+)^2}{\alpha^2}$, *which is a constant because the distribution of* $\bar{g}$ *is fixed within a round. With probability at most* $\frac{\diamond}{N_R^2}$, *we have* $\|\bar{g}_R - \mathbb{E}[\mu]\| \geq \|\bar{g} - \mathbb{E}[\mu]\|$.

Proof. We first derive the variance of $\bar{g}_R$ in two steps. First, $\bar{g}_R$ is the average of N_R updates. Therefore, we have the variance of the corresponding μ_R in State 1 of the hierarchical distribution in Assumption 2:

$$\mathrm{Var}[\mu_R] = \frac{1}{N_R^2}\mathrm{Var}[\mu]. \tag{30}$$

Then, in Stage 2, the gradient estimation process on each client adds variance to each μ_i and samples g_i. Since the variance of g_i is upper bounded by σ^+, we have

$$\mathrm{Var}[\bar{g}_R] \leq \frac{1}{N_R^2}(\mathrm{Var}[\mu] + \sigma^+). \tag{31}$$

Then, introducing an auxiliary variable α, with Chebyschev's inequality, we have:

$$\begin{aligned}
\mathbb{P}\Big[\|\bar{g}_R - \mathbb{E}[\mu]\| \geq \|\bar{g} - \mathbb{E}[\mu]\|\Big] &= \int_{\alpha=0}^{\infty} \mathbb{P}\Big[\|\bar{g}_R - \mathbb{E}[\mu]\| \geq \alpha\Big] \mathbb{P}\Big[\|\bar{g} - \mathbb{E}[\mu]\| = \alpha\Big] \\
&\leq \int_{\alpha=0}^{\infty} \mathbb{P}\Big[\|\bar{g} - \mathbb{E}[\mu]\| = \alpha\Big] \frac{(\mathrm{Var}[\mu] + \sigma^+)^2}{N_R^2 \alpha^2} \\
&= \frac{1}{N_R^2} \int_{\alpha=0}^{\infty} \mathbb{P}\Big[\|\bar{g} - \mathbb{E}[\mu]\| = \alpha\Big] \frac{(\mathrm{Var}[\mu] + \sigma^+)^2}{\alpha^2},
\end{aligned} \tag{32}$$

where $\int_{\alpha=0}^{\infty} \mathbb{P}\Big[\|\bar{g} - \mathbb{E}[\mu]\| = \alpha\Big] \frac{(\mathrm{Var}[\mu]+\sigma^+)^2}{\alpha^2}$ is a constant because the distribution of $\bar{g}$ is fixed within a round. □

C.16 Empirical Evaluation of Gradient Angles

We empirically explore conditions under which the $2\theta^* \leq \theta$ case and the general cases in Figure 2 happen on the FEMNIST dataset. Our experiments include 10%, 20%, 30%, 40%, 50%, 60%, 70%, and 80% adversaries. We find that the $2\theta^* \leq \theta$ case happens with 30% - 80% adversaries and the general case happens with 10% - 20% adversaries.